# Lecture 5

# CME Flux Ropes

February 1, 2017

# energy release on the Sun in a day

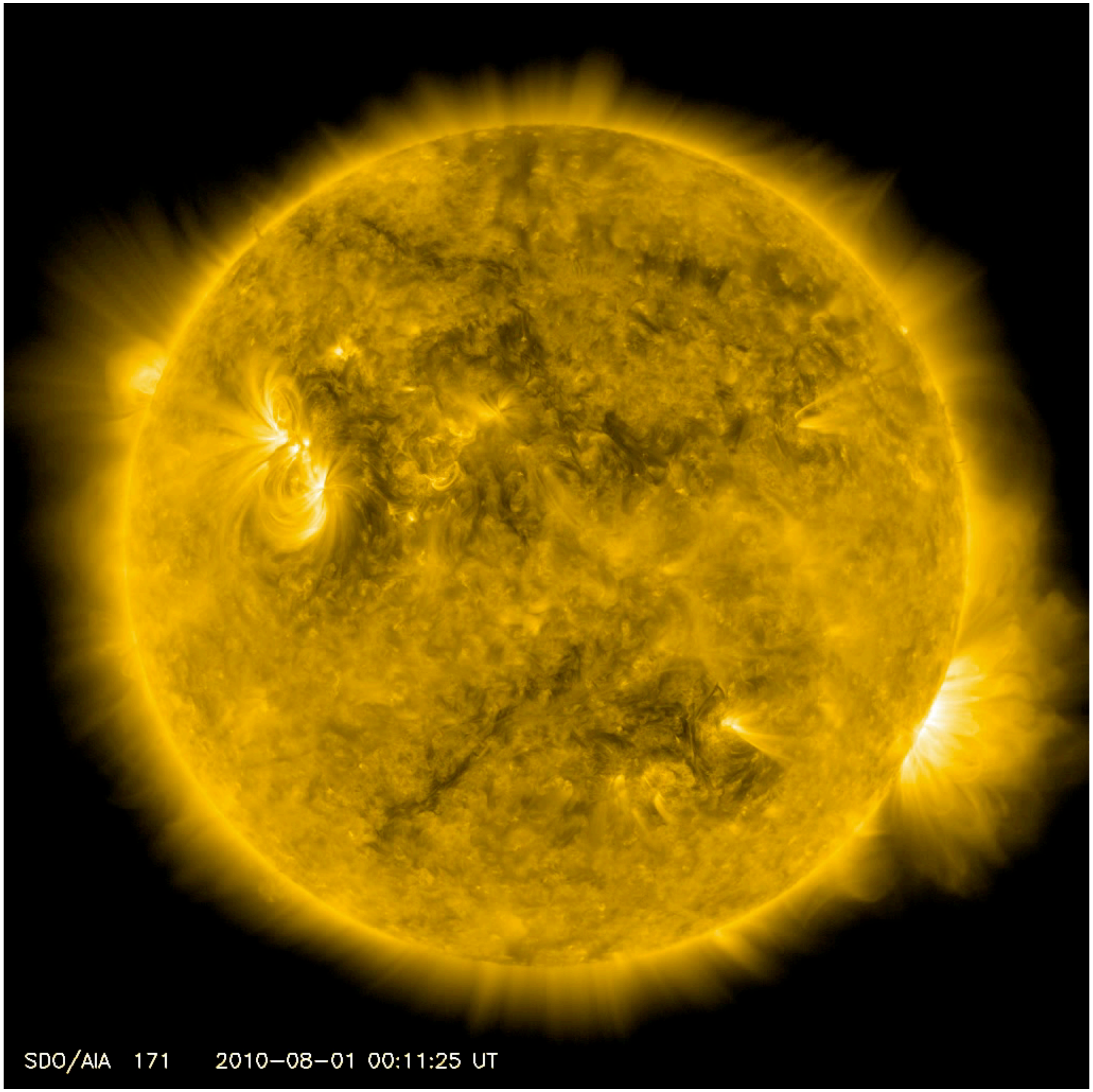

# CMEs best seen by coronagraphs – LASCO C2

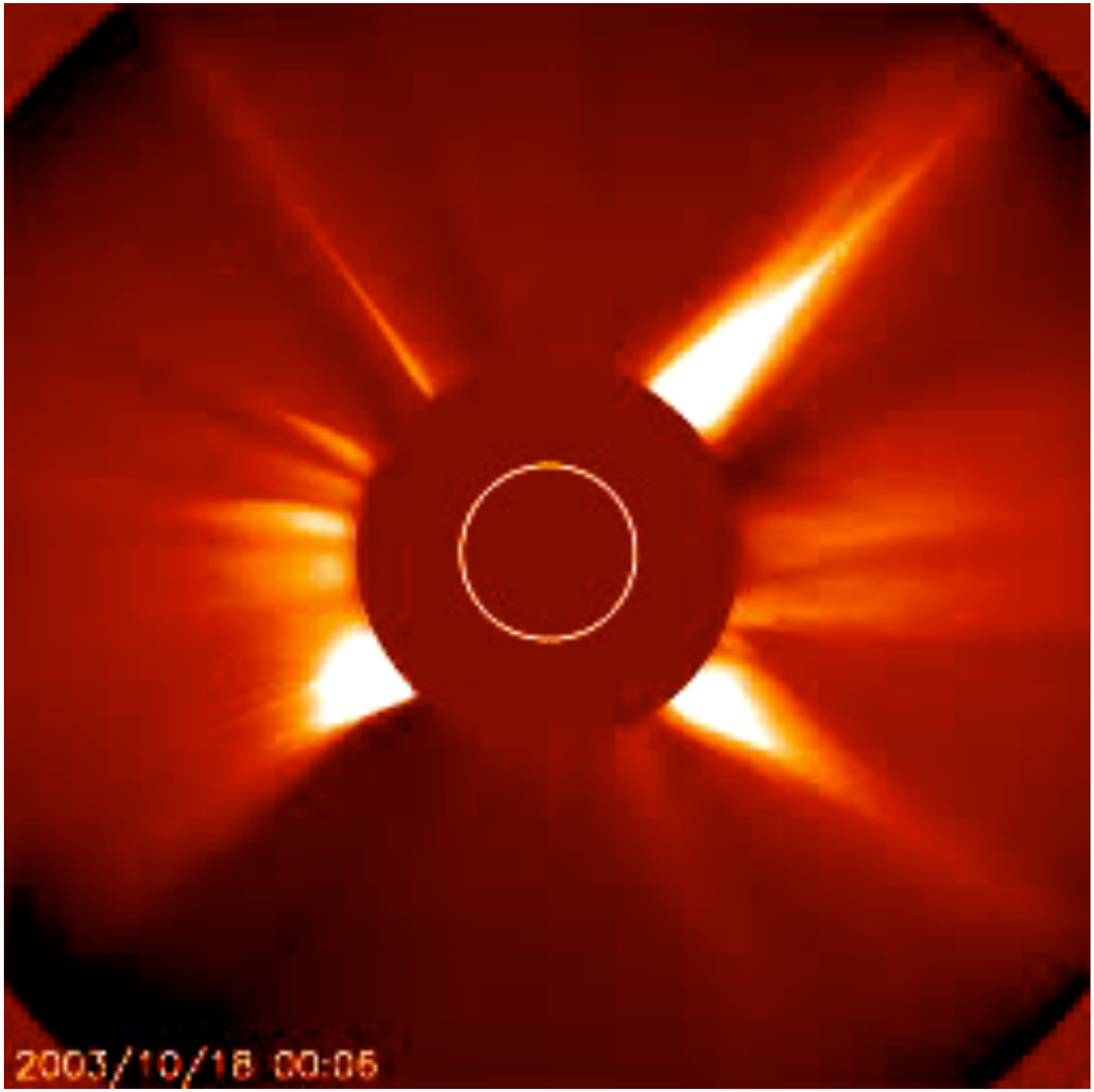

# CMEs best seen by coronagraphs – LASCO C3

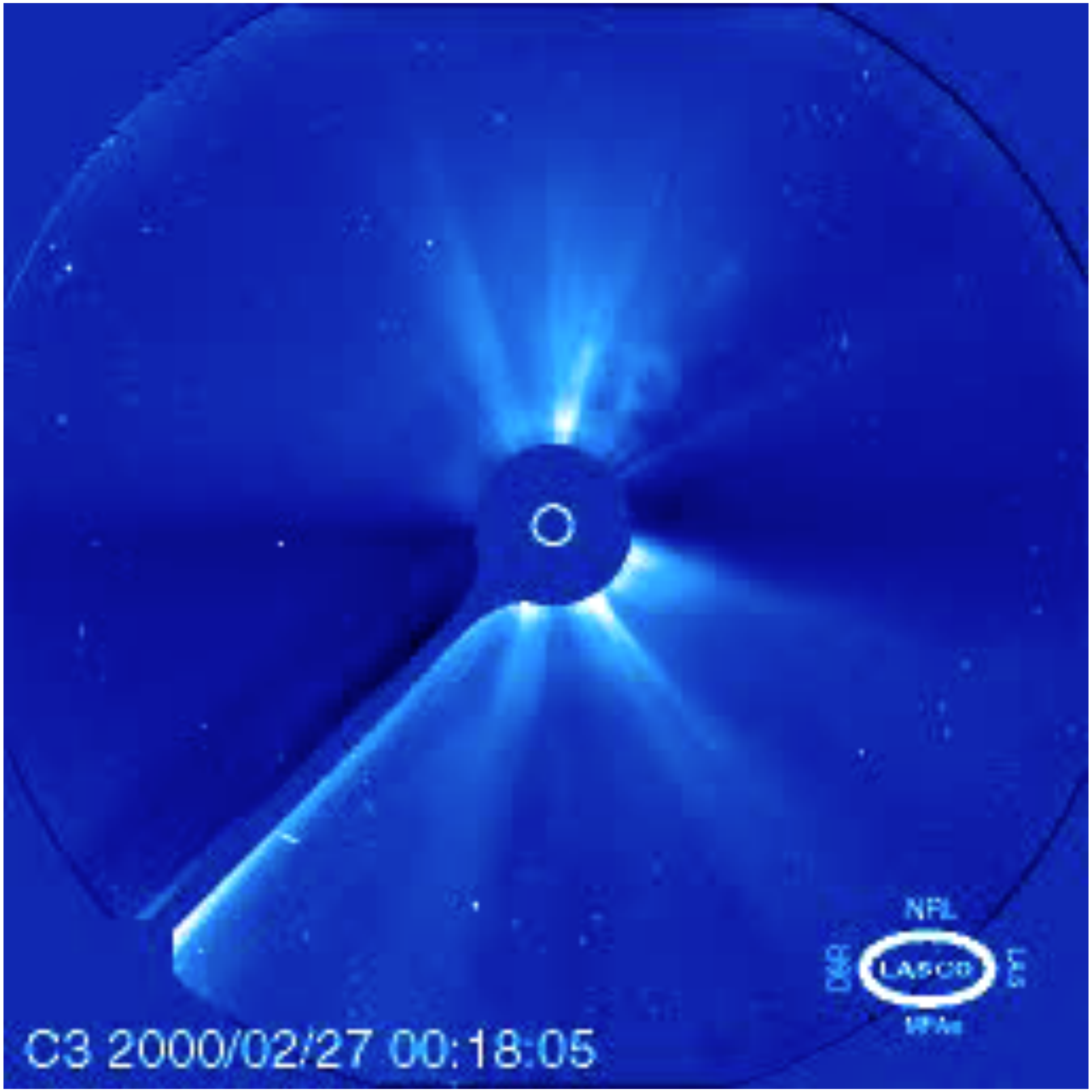

# The three-part white light CME

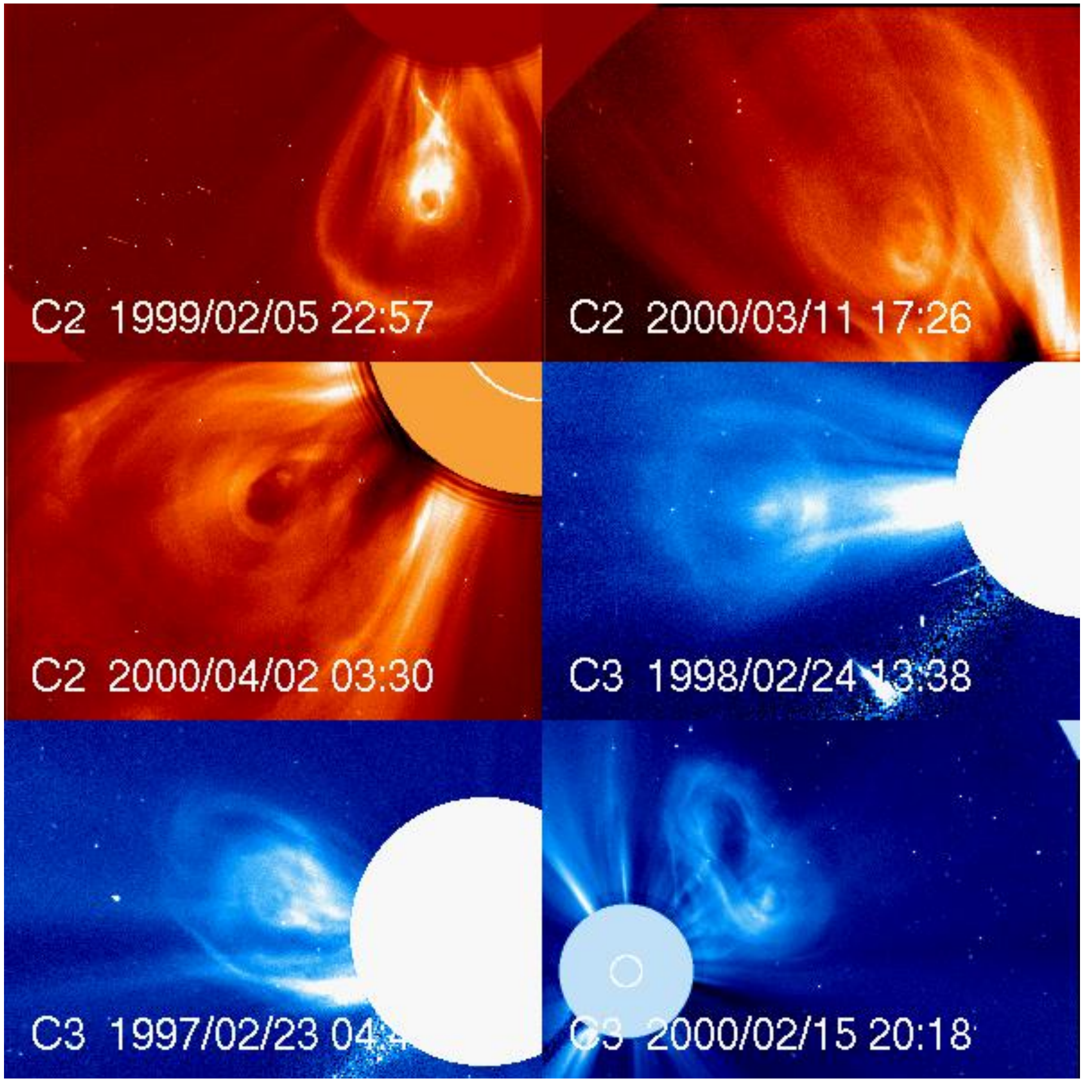


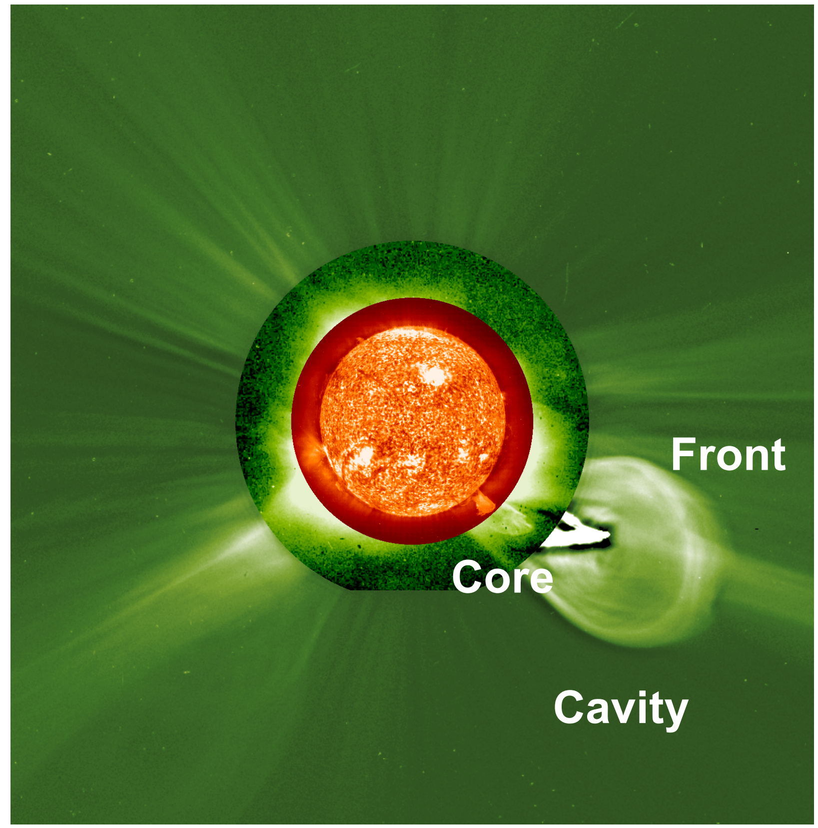


Vourlidas et al 2013

# standard flare-CME model

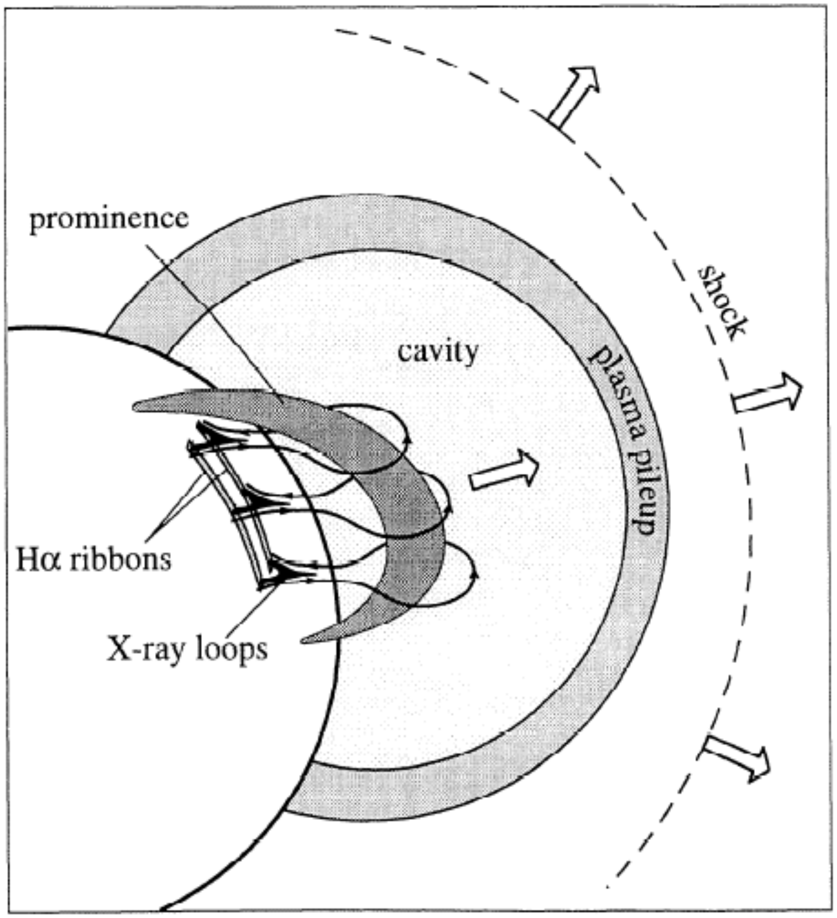


Forbes-Lin model

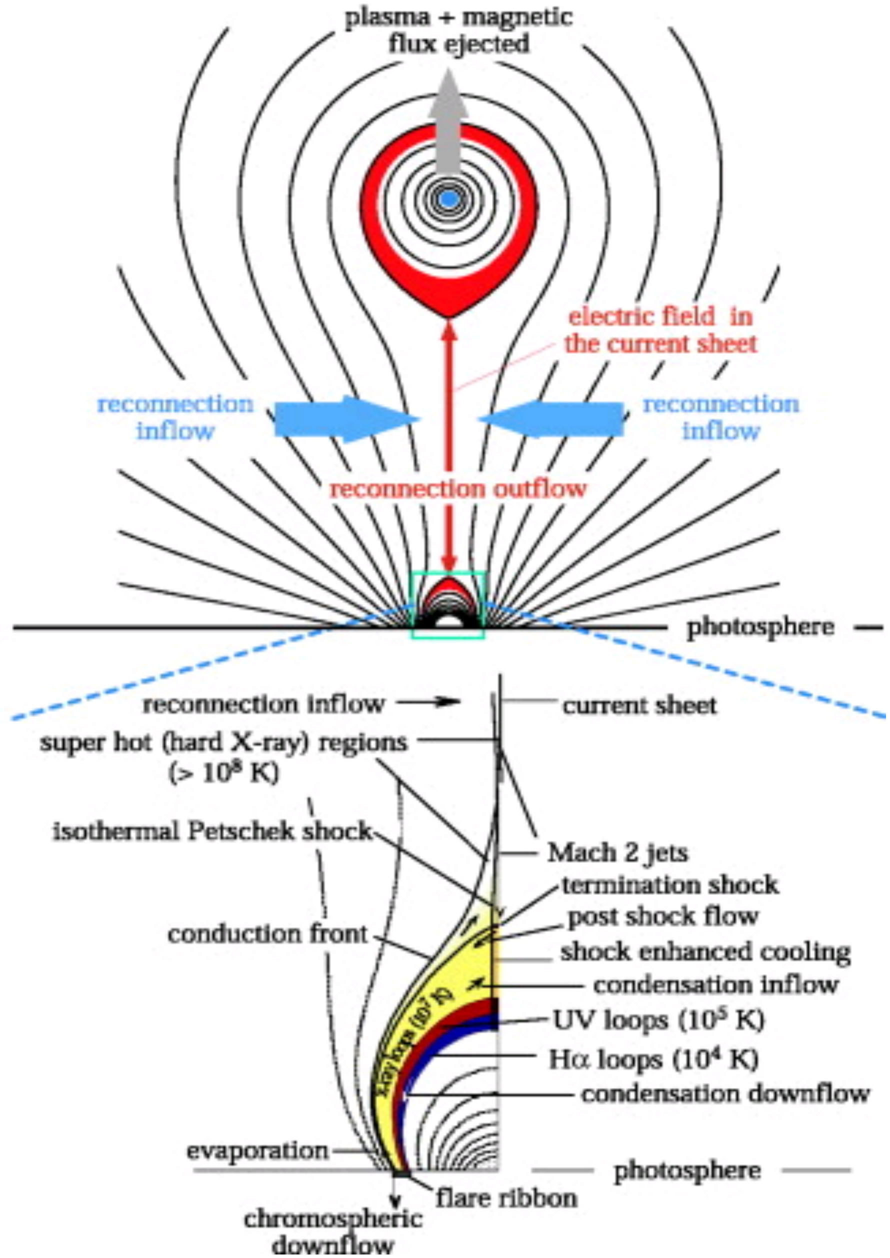

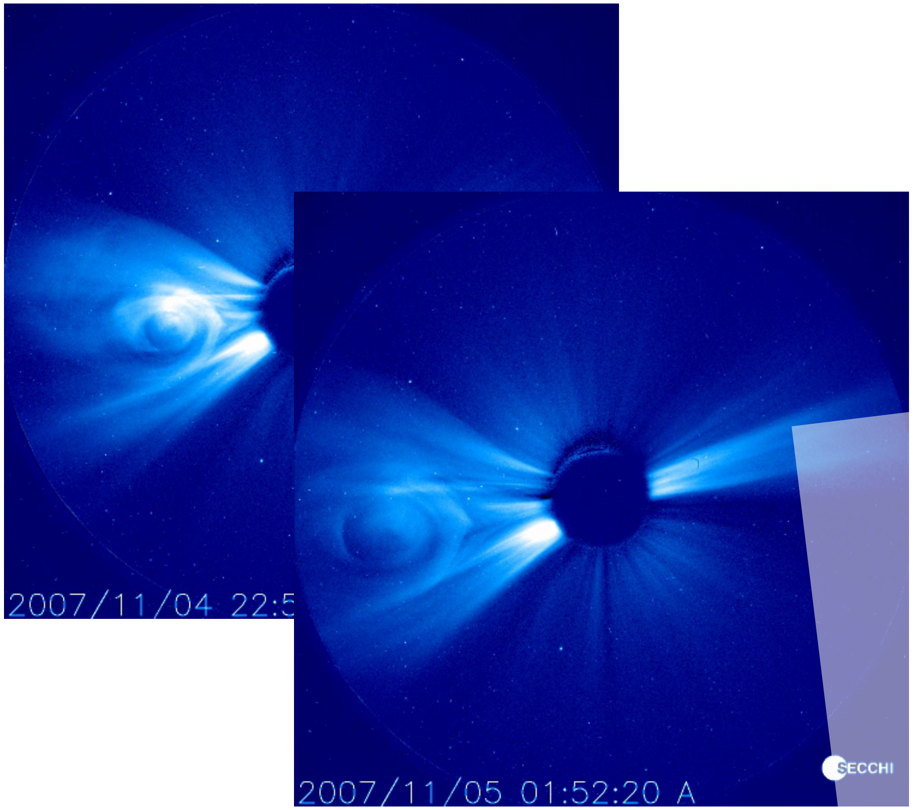


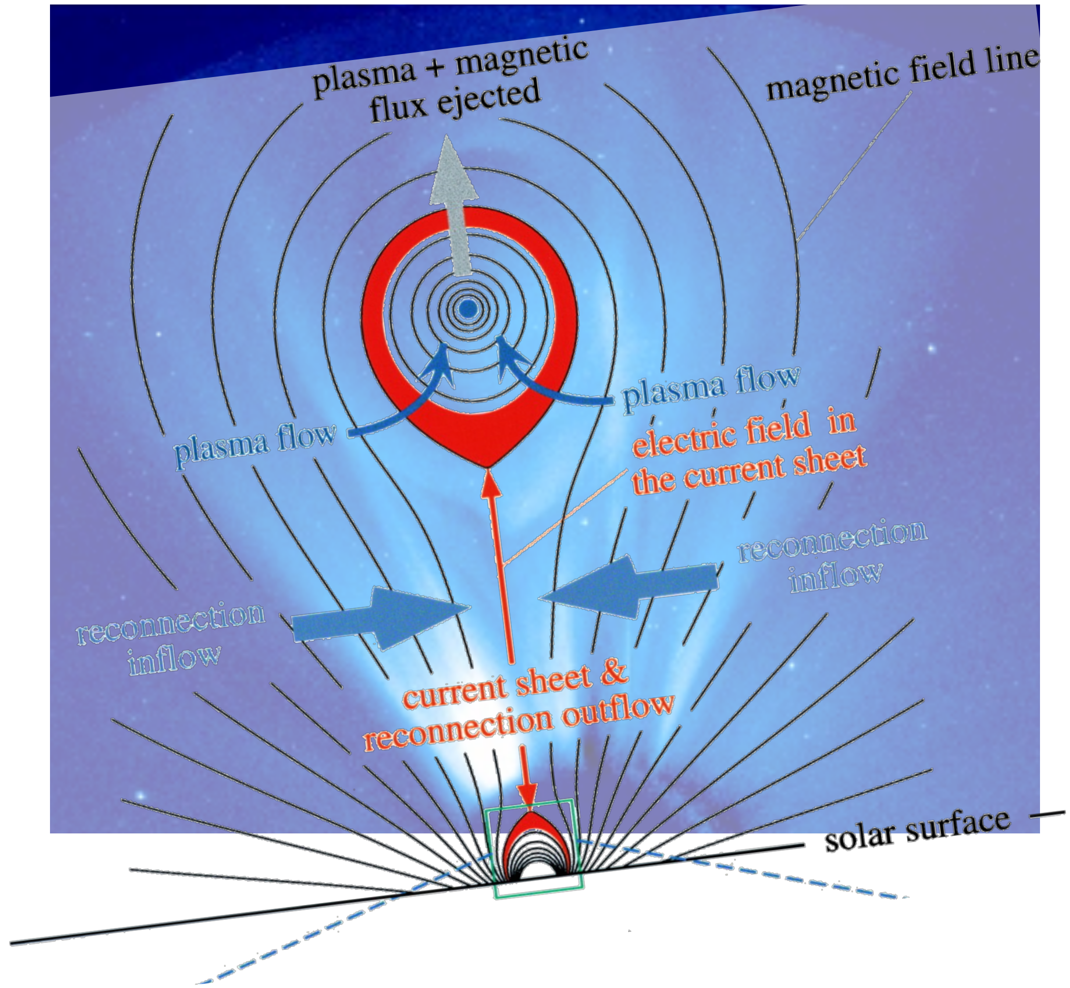


1. structure
2. genesis
3. energetics

# Brief History of Magnetic Cloud

- 1954 Morrison: unusual magnetized clouds of plasma emitted by the active sun.
- 1958 Cocconi et al.: magnetic loop or bottle anchored in the sun.
- 1958 Piddington: magnetic bubble detached from the sun by reconnection.
- 1959 Gold: shocks preceding these magnetic loops
- 1980-81 Burlaga: first coined "magnetic cloud"
- 1990, 1997, Lepping: magnetic cloud properties

(Burlaga et al, 1981, JGR, 86, 6673-6684)

# In-situ measurements of Magnetic Cloud

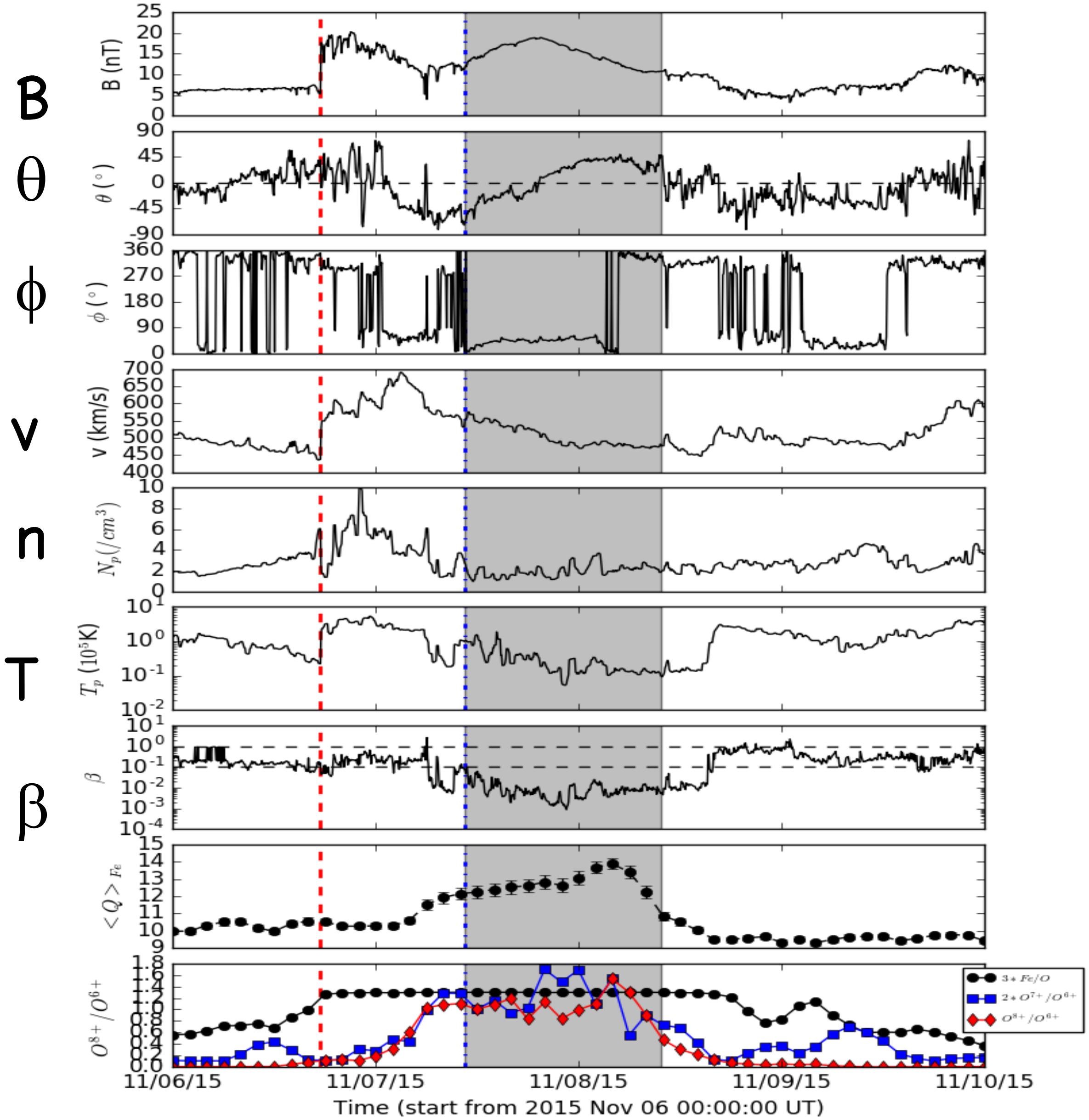


Liu R. et al. 2017

Tightly wound helix
B: 10 - 100 nT

Low temperature and plasma density
T : $10^5$ K, n: 10 – 100 $cm^{-3}$, β: 0.01 – 0.1

Higher speed than ambient solar wind
v: 300 - 800 km $s^{-1}$

Preceded by shocks and sheaths

(Burlaga et al 1981; Lepping et al. 1990)

# In-situ measurements of Magnetic Cloud

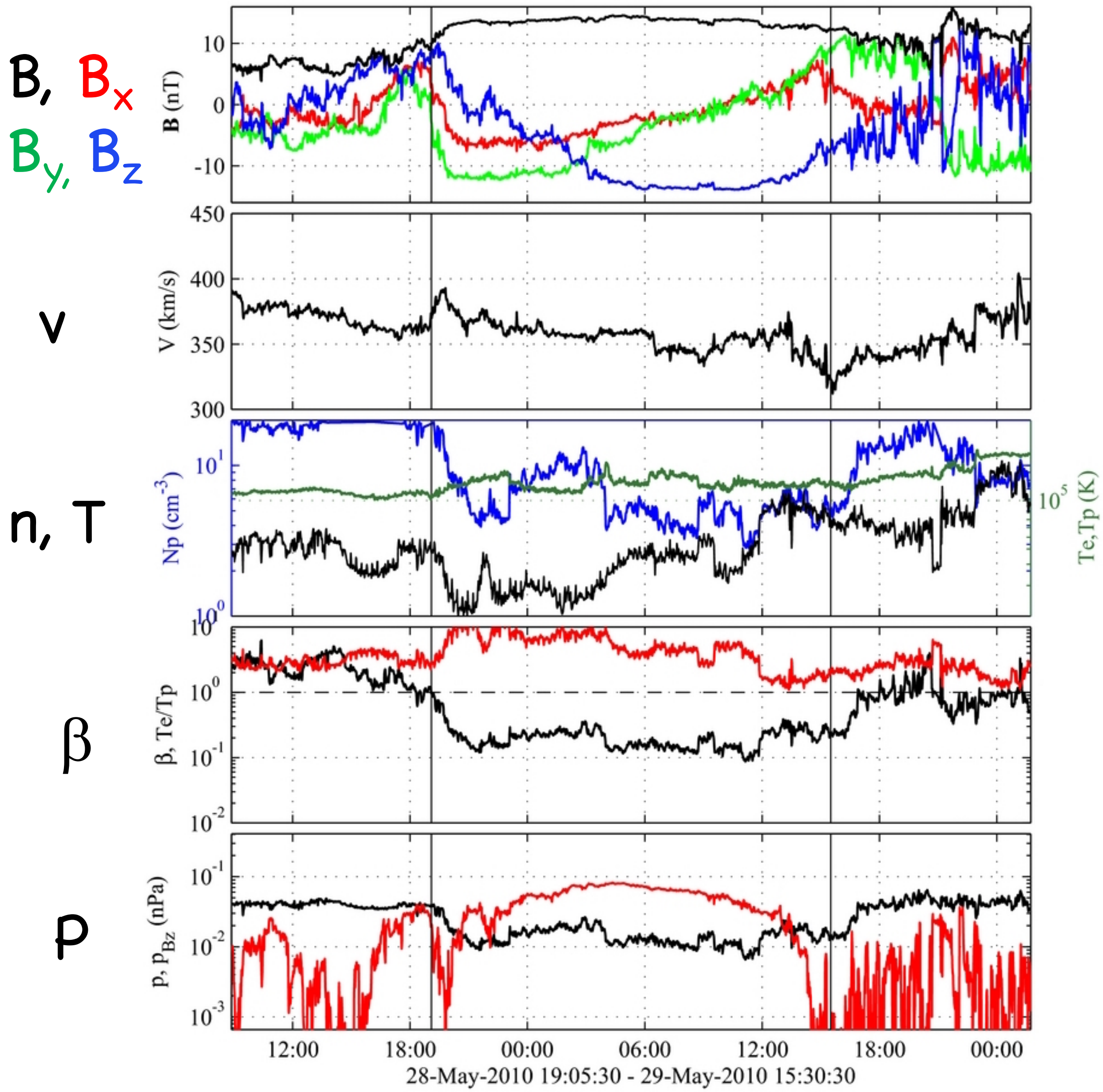


Hu et al. 2014

Tightly wound helix
B: 10 – 100 nT

Low temperature and plasma density
T : $10^5$ K, n: 10 – 100 $cm^{-3}$, $\beta$: 0.01 – 0.1

Higher speed than ambient solar wind
v: 300 – 800 km $s^{-1}$

Preceded by shocks and sheaths

(Burlaga et al 1981; Lepping et al. 1990)

# Magnetic Cloud: interplanetary flux rope

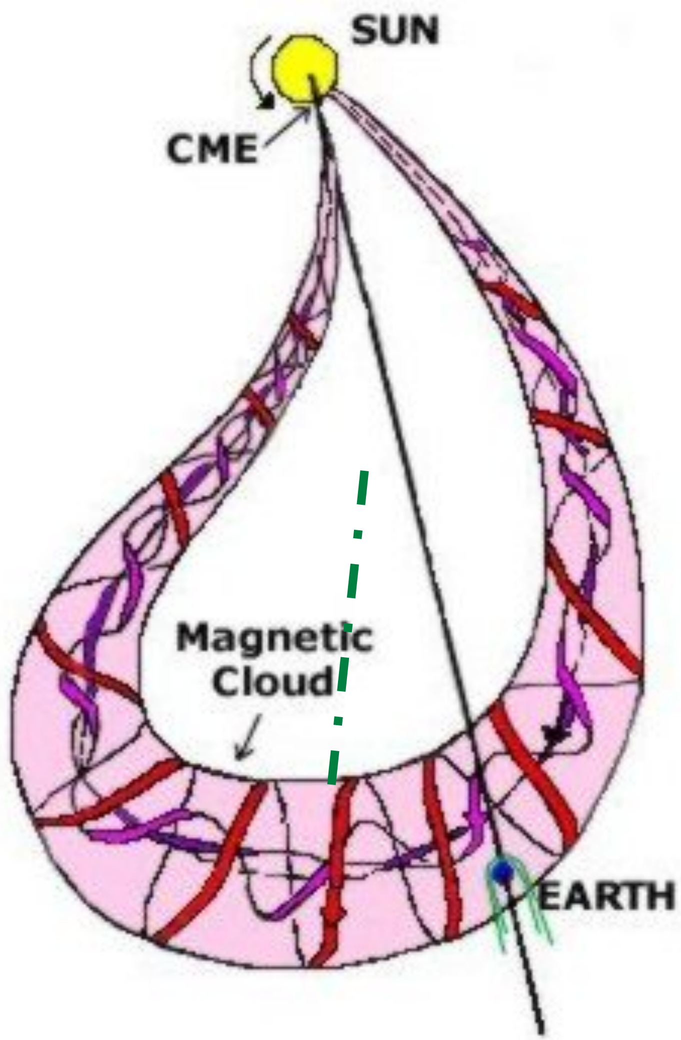

[After Marubashi]

Not to Scale

From in-situ observations, a flux rope may be reconstructed with various methods (Riley et al. 2004, Dasso et al. 2006 for a summary of these methods), assuming a 2d cylindrical structure of the CME flux rope.

# MC flux rope: the Lundquist solution

$$\mathbf{B}_0(r) = B_0\left[J_0(\alpha r)\hat{\mathbf{z}} + J_1(\alpha r)\hat{\phi}\right]$$

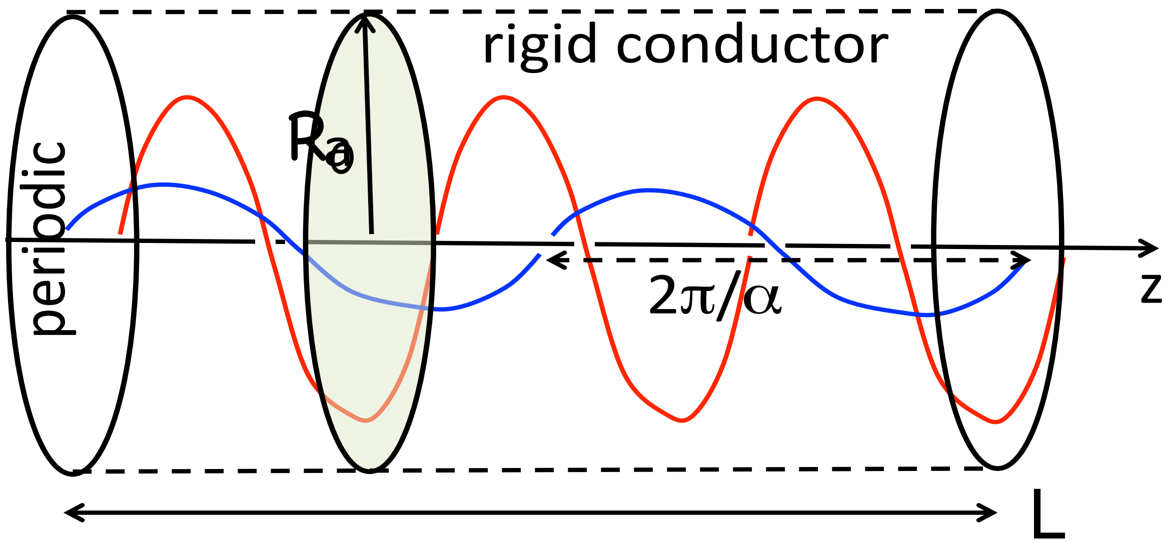


Least-squares fitting of the data points to determine 7 parameters, including the rope axis orientation, radius, and axial field $B_0$.

(Lepping et al. 1990, Lynch et al. 2005)

toroidal flux:

$$\Phi_t = \iint B_z r dr d\phi$$

poloidal flux:

$$\Phi_p = \iint B_\phi \, dr dl$$

magnetic helicity:

$$H_m = \int \vec{A} \cdot \vec{B} \, d^3x$$

$$= \frac{1}{\alpha}\int B^2 d^3x$$

magnetic twist:

$$T = \frac{lB_\phi}{rB_z}, \quad \tau = \frac{T}{2\pi}$$

# MC flux rope: the Lundquist solution

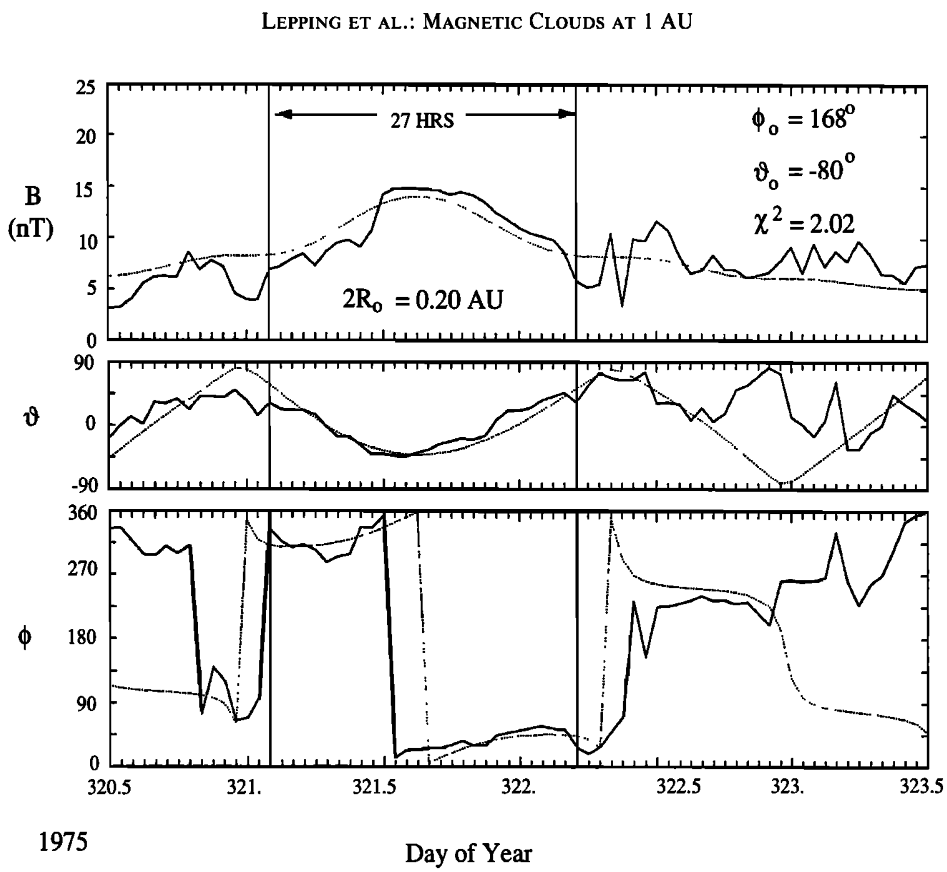


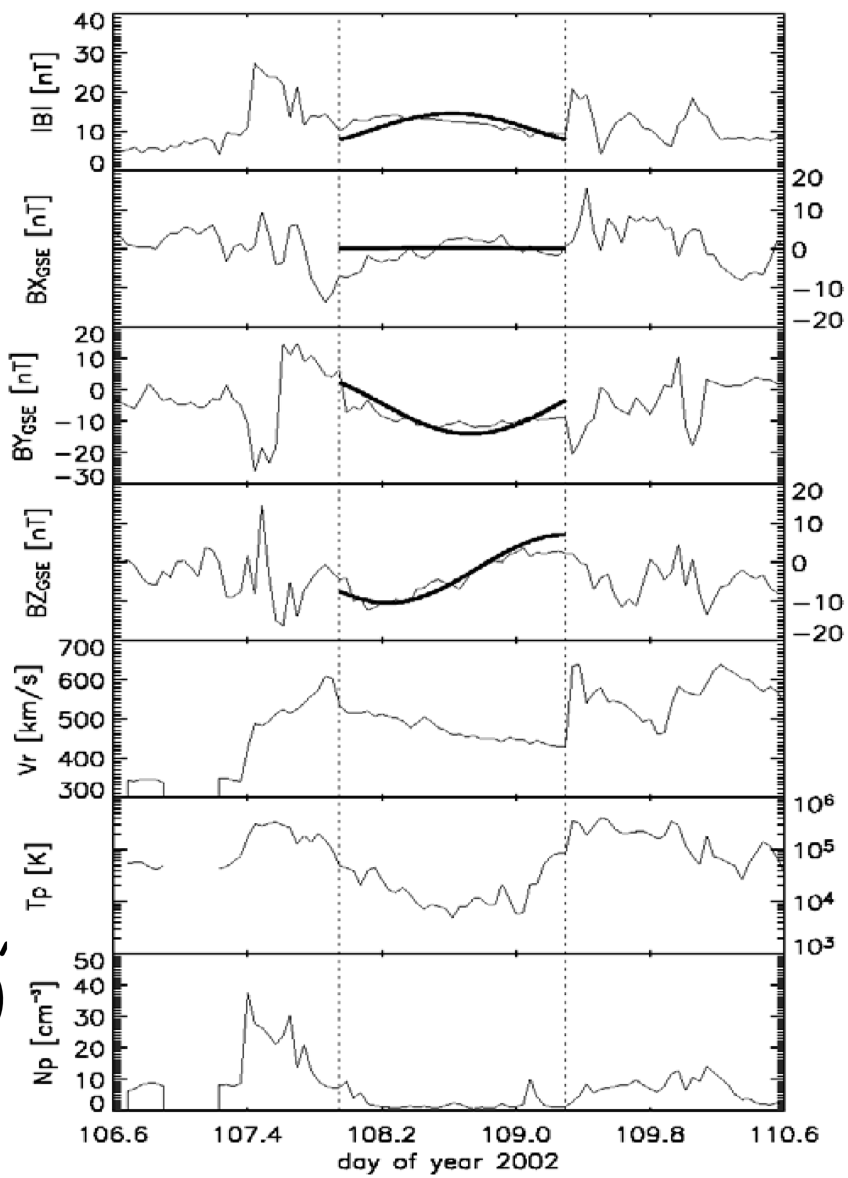


18 MC flux ropes by Lepping et al. 1990, and 132 MC ropes by Lynch et al. 2005)

# MC flux rope: the GS solution

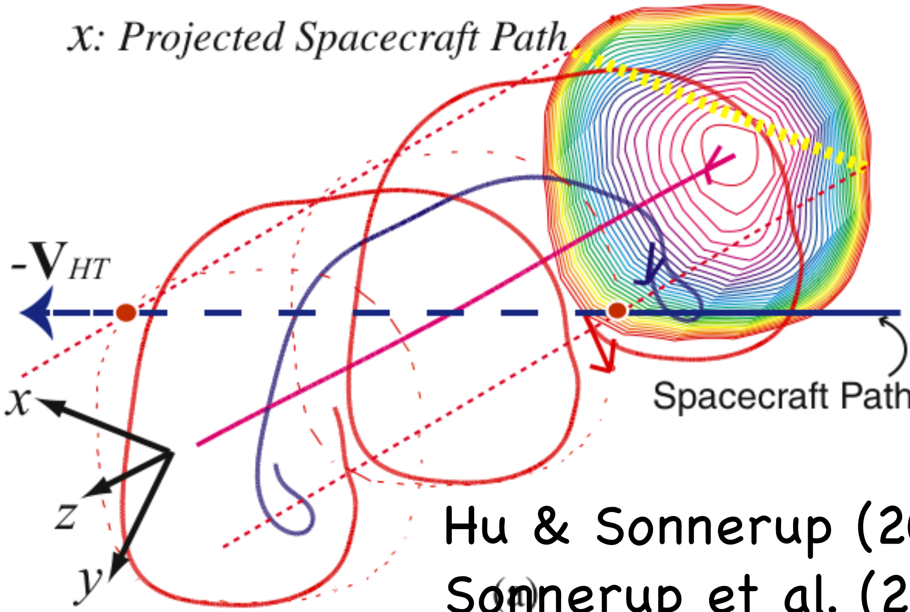


Hu & Sonnerup (2002)
Sonnerup et al. (2006)

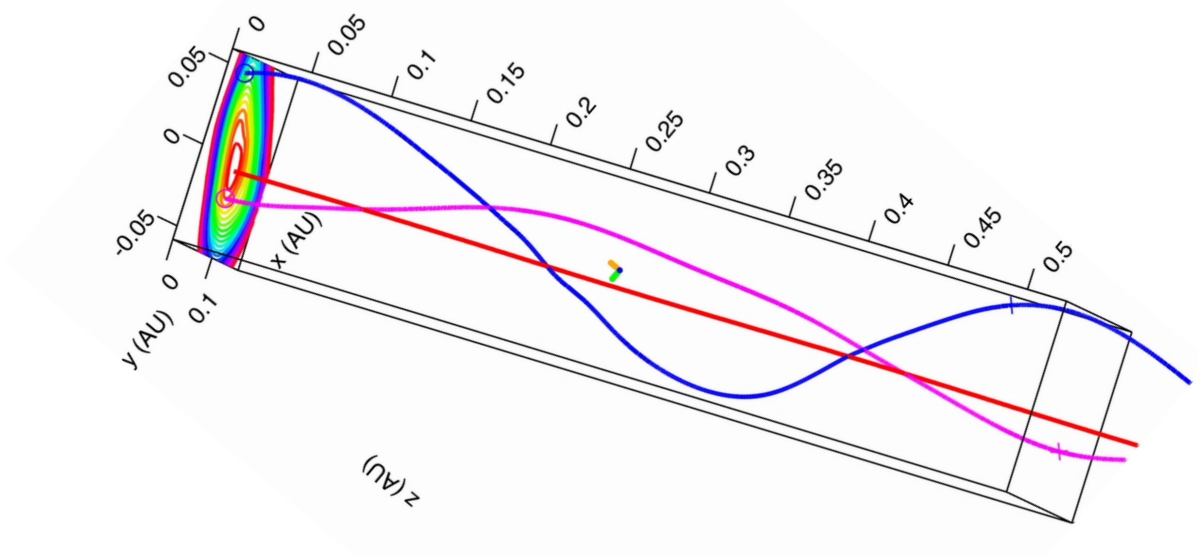


2d magnetostatic non-force-free Grad-Shafranov equation

$$\vec{\nabla} p = \vec{j} \times \vec{B}$$

$$\vec{B} = \left( \frac{\partial A}{\partial y}, -\frac{\partial A}{\partial x}, B_z(A) \right)$$

$$P_t(A) = p(A) + B_z^2 / 2\mu_0$$

$$\frac{\partial^2 A}{\partial x^2} + \frac{\partial^2 A}{\partial y^2} = -\mu_0 \frac{dP_t}{dA}$$

$$\Phi_t = \iint B_z dxdy$$

$$\Phi_p = |A_m - A_b| L$$

$$\tau = 1AU/Lz$$

# MC flux rope: the GS solution

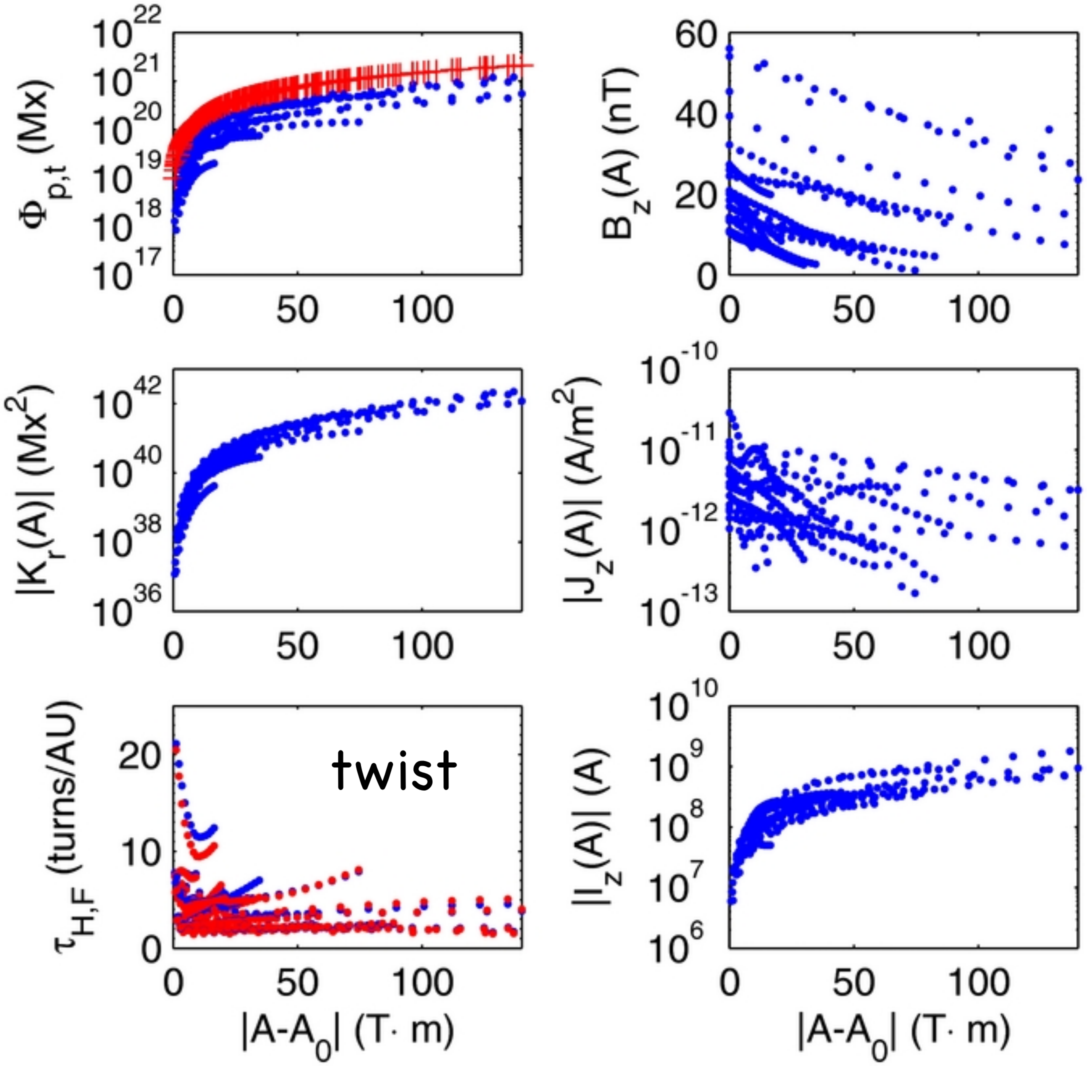


18 MC flux ropes by Hu et al. (2014)

MC flux ropes carry an average twist of $\tau$ > 3 per AU. Most of them deviate from the Lundquist solution (Hu et al. 2014, 2015; Kahler et al. 2011).

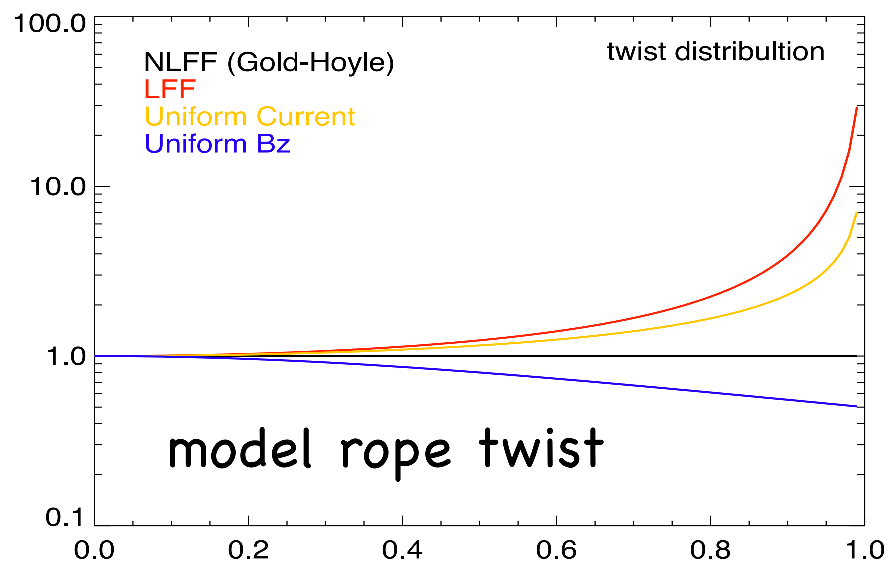

# Field line length of MC flux rope

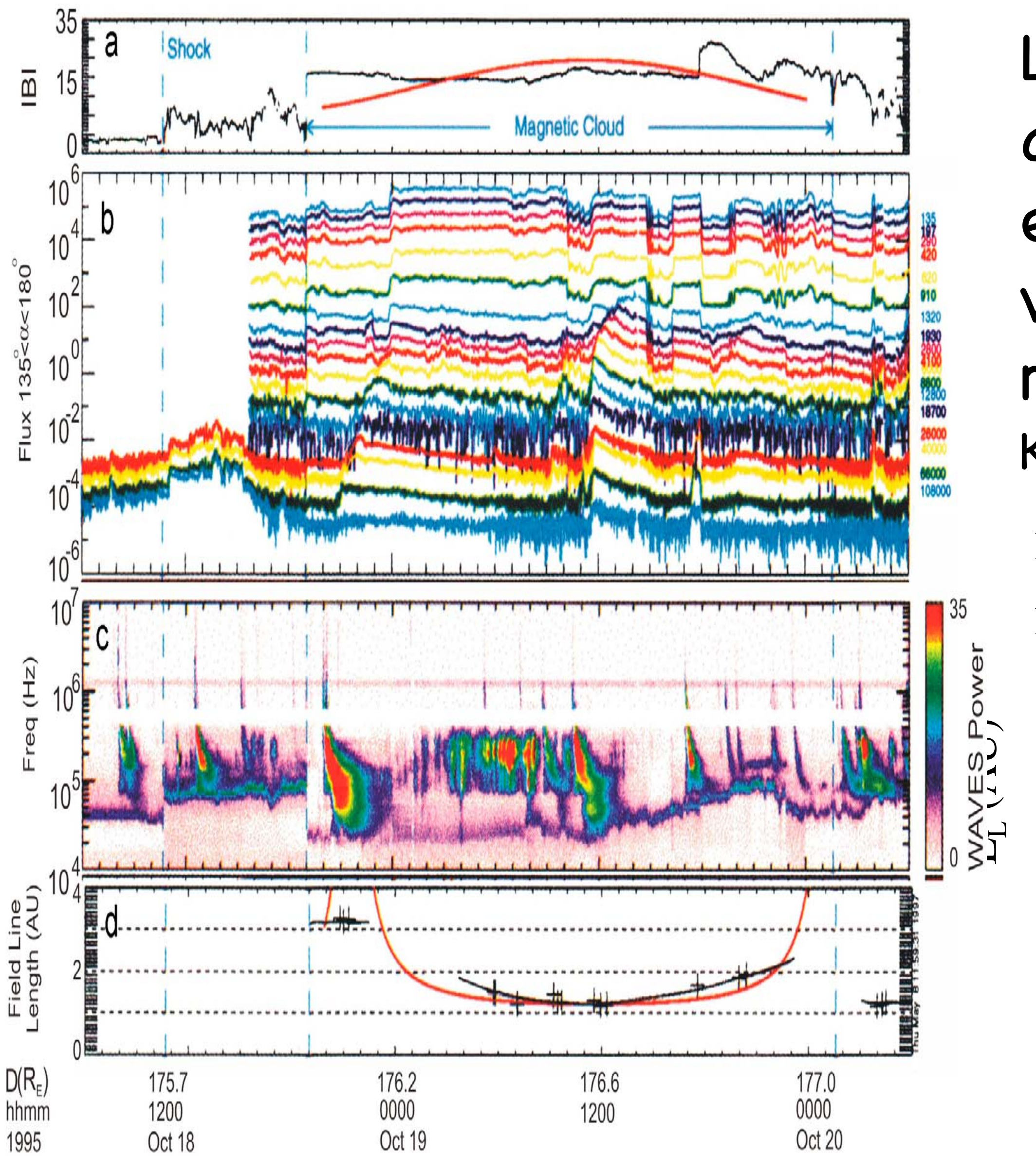


Figure 1. Composite panel of particles and fields measurements on the Wind spacecraft in the 18–20 October

Lengths of MC field lines are also measured from electron travel times, $L_e = v_e \Delta t$, to compare with models (Larson et al 1997, Kahler et al 2011, Hu et al. 2015)

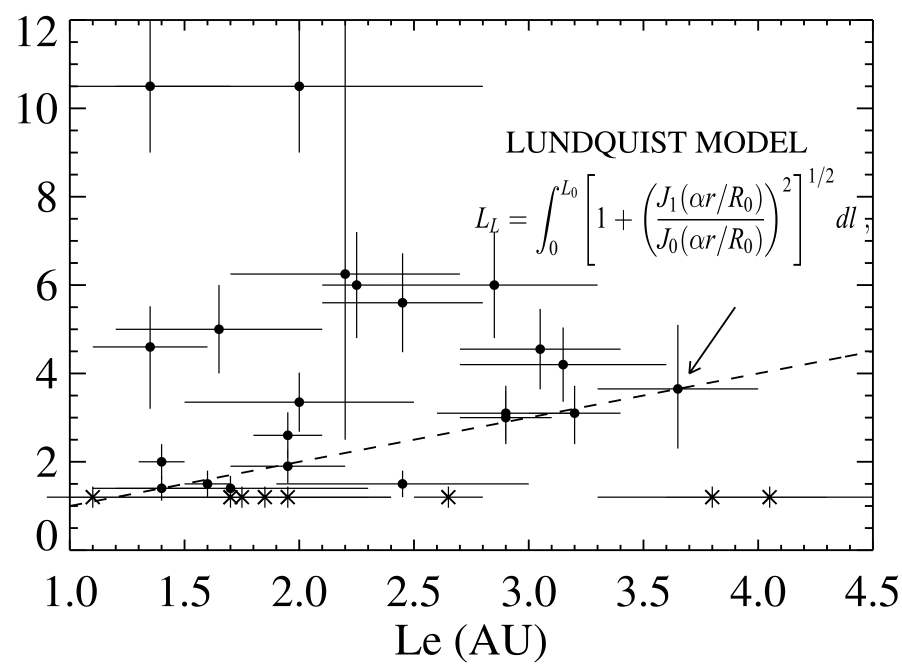

# properties of MC flux ropes

| property | typical values at 1 AU |
|---|---|
| cross-sectional radius (a) | 0.1 – 0.5 AU |
| axial (toroidal) flux | $10^{19-21}$ Mx |
| azimuthal (poloidal) flux per AU | $10^{20-22}$ Mx |
| magnetic helicity per AU | $10^{40-44}$ $Mx^2$ |
| magnetic twist per AU | 3 – 5 turns, or more |

(Lepping et al. 2000, Lynch et al. 2005, Kahler et al. 2011, Hu et al. 2014)

How are flux ropes formed?

# association with solar source regions

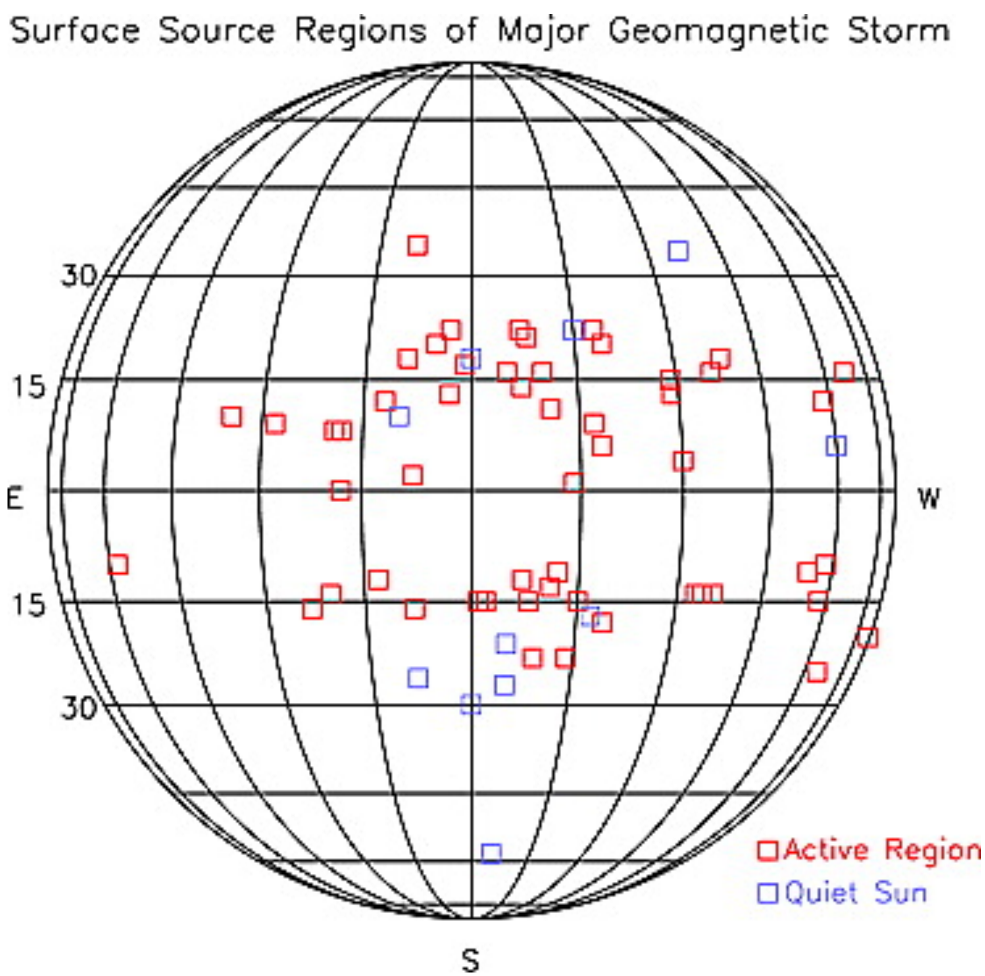

Zhang et al. (2007)

CDAW (1996-2005) identified solar source for 88 geomagnetic storms (Dst < -100 nT), 46 being MCs.

| # of MCs (46) | Solar Source |
|---|---|
| 28 (61%) | Active Regions |
| 8 (17%) | Quiet Sun |
| 10 (22%) | unknown |

# genesis of a flux rope

The debate on nature or nurture: the flux rope is born from below the photosphere (emerging flux rope), or is made in the corona, by reconnection, during its eruption (in-situ formed flux rope), or a hybrid of the two.

| | **Pre-existing rope** | **In-situ formed rope** |
|---|---|---|
| idea | Formed in convection zone, emerges to the corona, or formed in the corona, but **prior to** eruption | Formed in-situ **during** eruption by magnetic reconnection |
| models | Chen89, Low96, Gibson98, Fan04, Forbes-Priest-Isenberg-Lin, VanBallegooijen89 | Moore80, Mikic88, Mikic94, Choe96, Demoulin96, Titov99, Antiochos99, Amari03, Longcope07 |
| observations | filaments, sigmoids, other indirect signatures. | sheared arcades, other indirect signatures. |
| problems | cannot measure magnetic field in the corona | cannot measure magnetic field in the corona |

# examples of a pre-existing flux rope

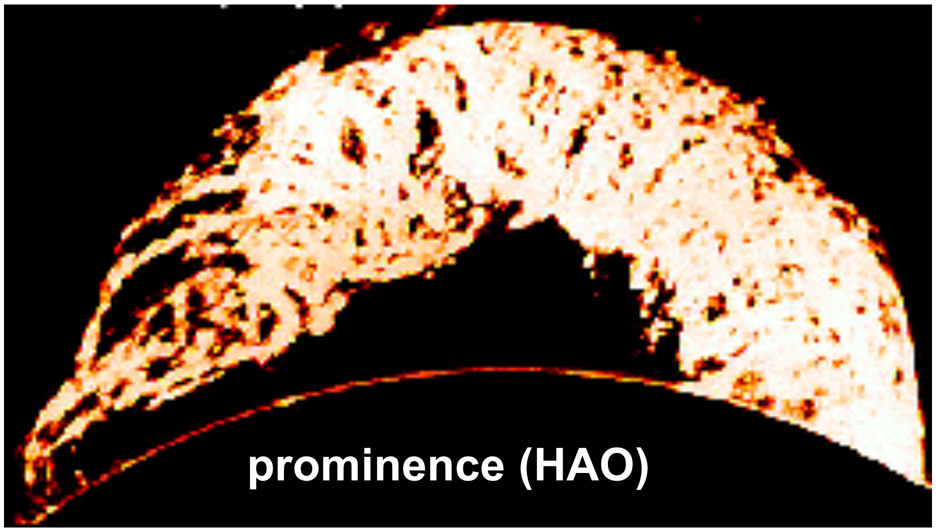


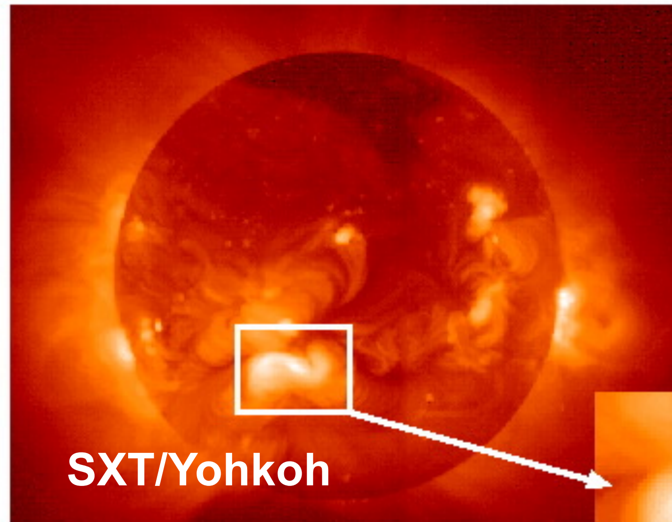


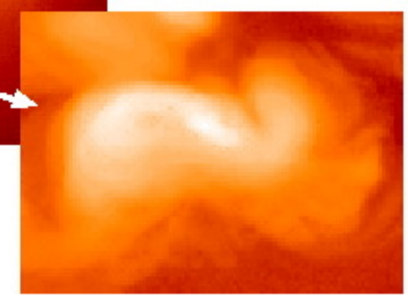

SXR sigmoid

Canfield et al. 2000

Filaments and sigmoids are magnetized plasma structures present prior to eruption with higher chance of MC occurrence.

# infer flux rope properties from surface signatures

| Physical property | Surface signatures | research |
|---|---|---|
| dynamics | CME speed | Gopalswamy01 |
| orientation, handedness | global magnetic field<br>loop arcade<br>filament<br>Sigmoid<br>dimming | Mulligan00<br>McAllister98<br>Rust94, Bothmer98<br>Canfield99, Pevtsov01<br>Webb00 |
| axial (toroidal) flux | active region<br>filament<br>dimming | Leamon04<br>Lepping97<br>Webb00 |
| azimuthal (poloidal) flux, electric current, helicity | active region<br>dimming<br>CME/flare<br>flare | Demoulin02, Nindos03, Leamon04<br>Mandrini05, Attrill06<br>Moore07<br>Longcope07, Qiu07, Kazachenko09,12 |

# flux ropes formed by reconnection

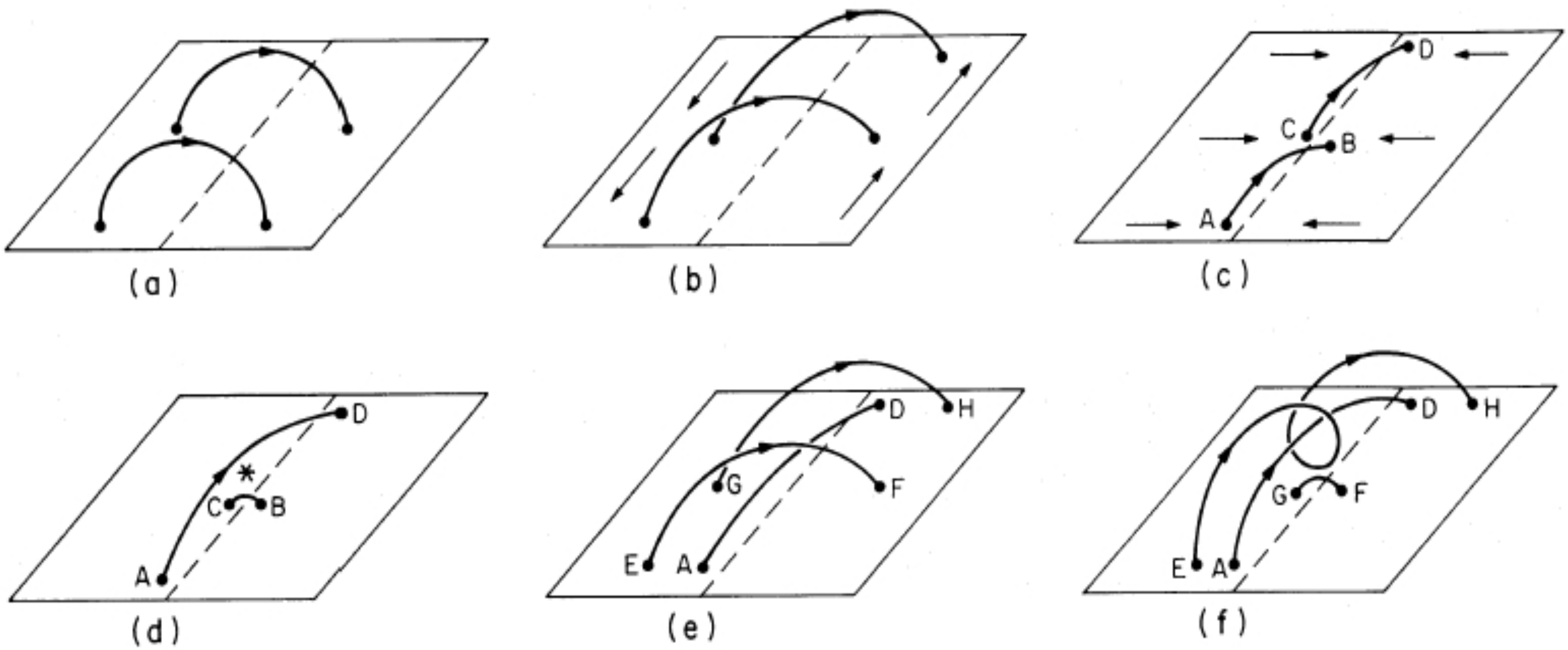


van Ballegooijen & Martens (1989)

Flux rope formed by magnetic reconnection of a sheared arcade, transferring shear to twist.

poloidal or azimuthal magnetic flux $\Phi_p$: the amount of **twist** along the field lines

flux rope formed by reconnection

The helical structure, or the **twist**, results from magnetic reconnection.

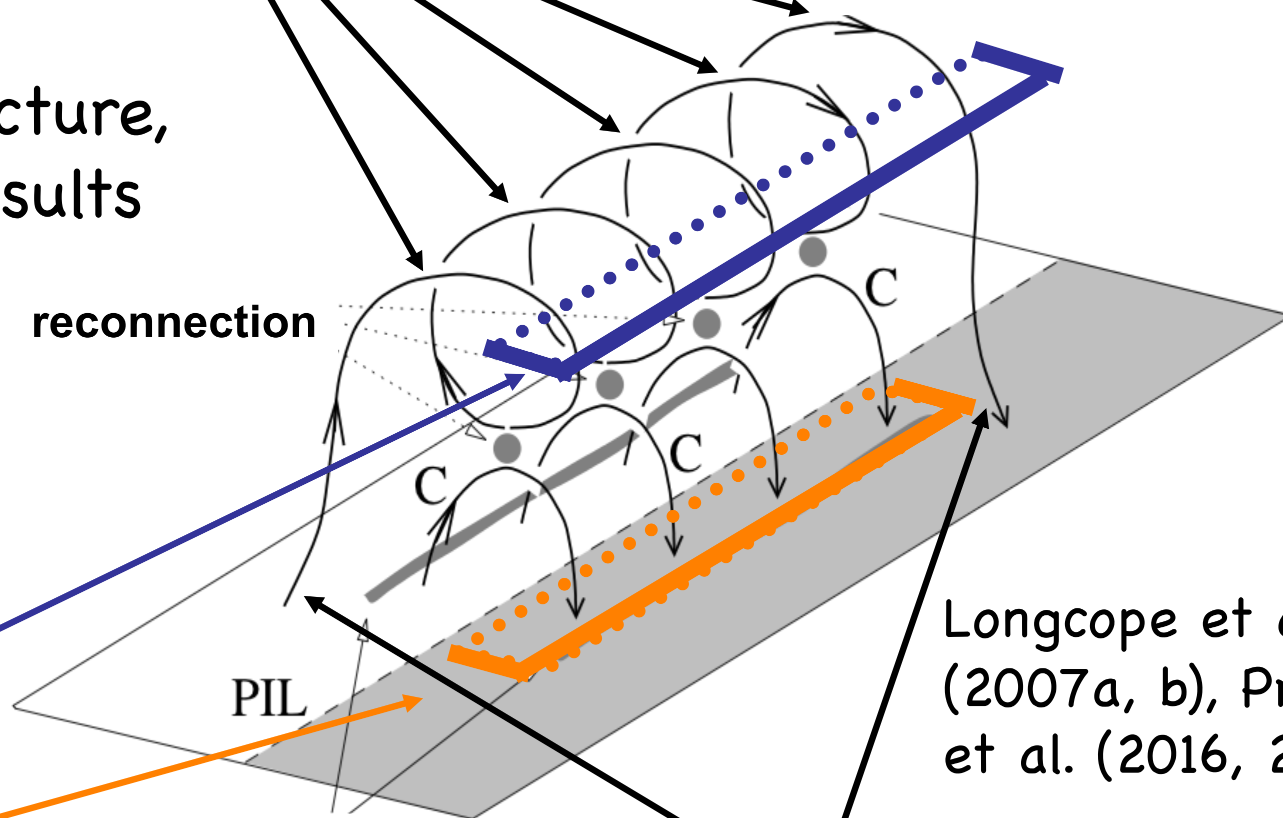


poloidal flux

reconnection flux $\Phi_r$

Longcope et al (2007a, b), Priest et al. (2016, 2017)

toroidal or axial magnetic flux $\Phi_t$

# reconnection is “visible” in disk observations

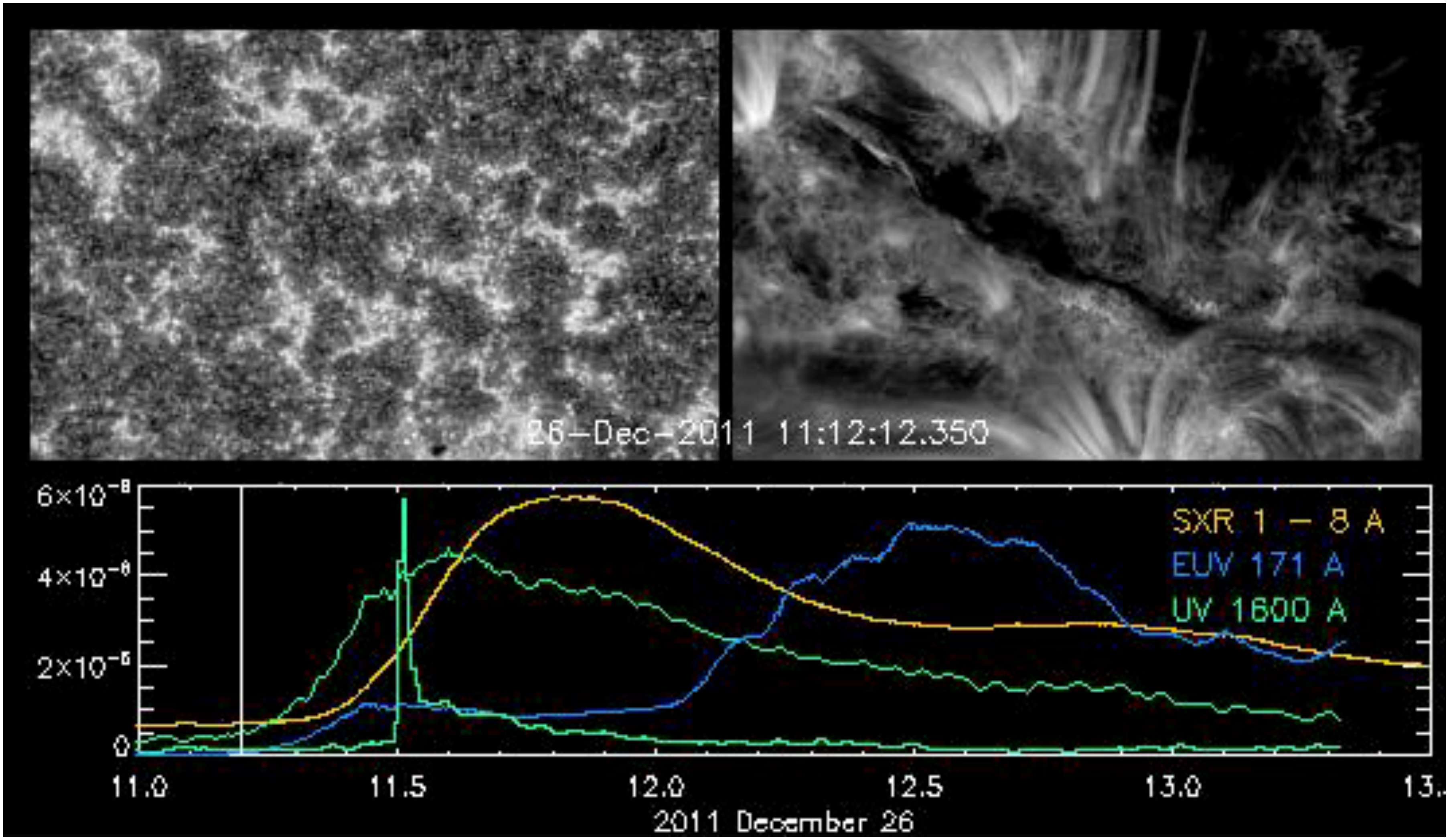


Flare loops and their foot-points are bright because of plasma heating along post-reconnection flux tubes.

# reconnection is measured from flare ribbons

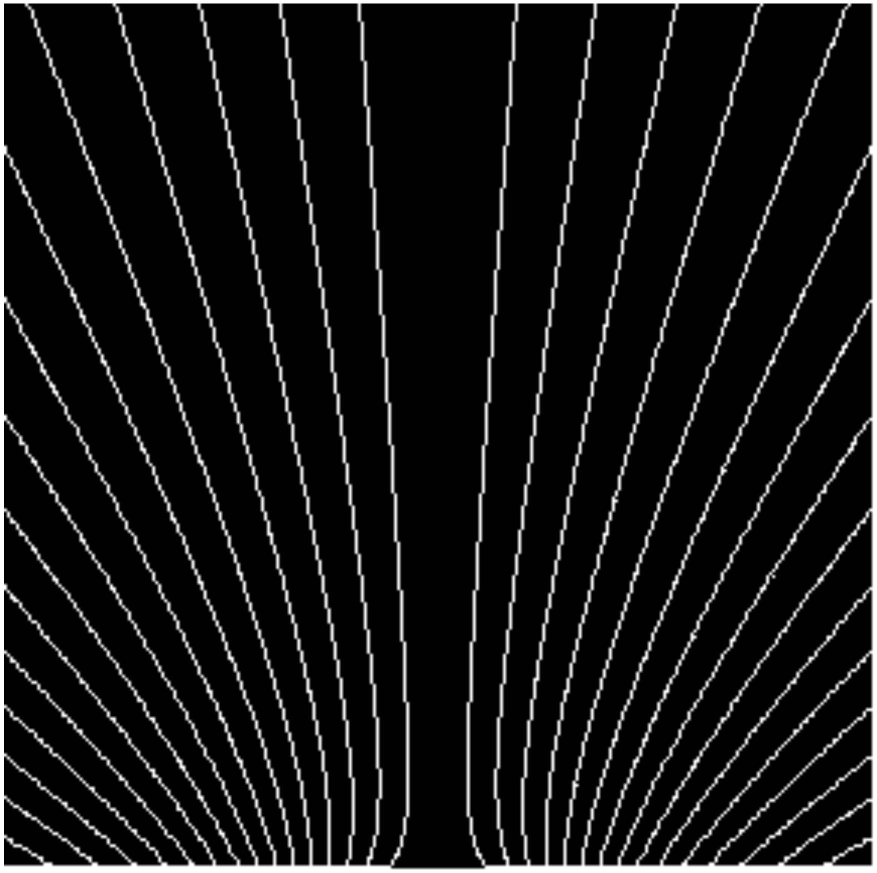

(Terry Forbes)

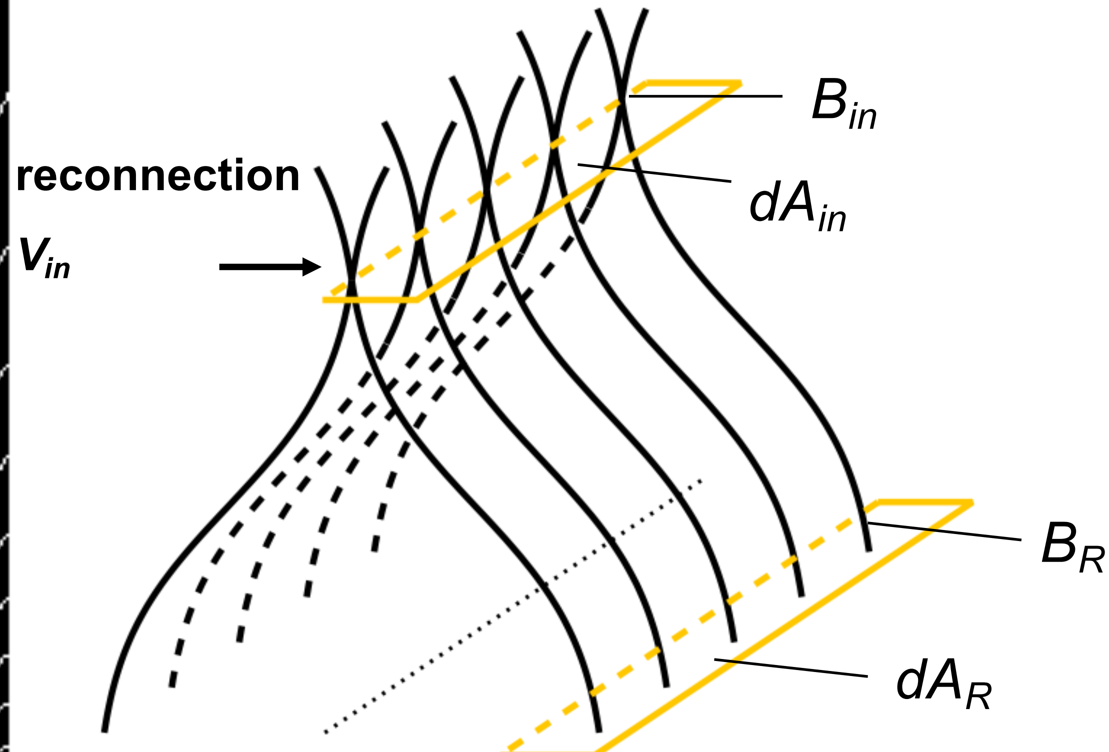


$$\frac{d\Phi_B}{dt} = -\oint \vec{E} \bullet d\vec{l} = \frac{d}{dt}\left(\int B_{in} dA_{in}\right) = \frac{d}{dt}\left(\int B_R dA_R\right)$$ (Forbes & Priest 1984)

# by mapping ribbons on the magnetogram

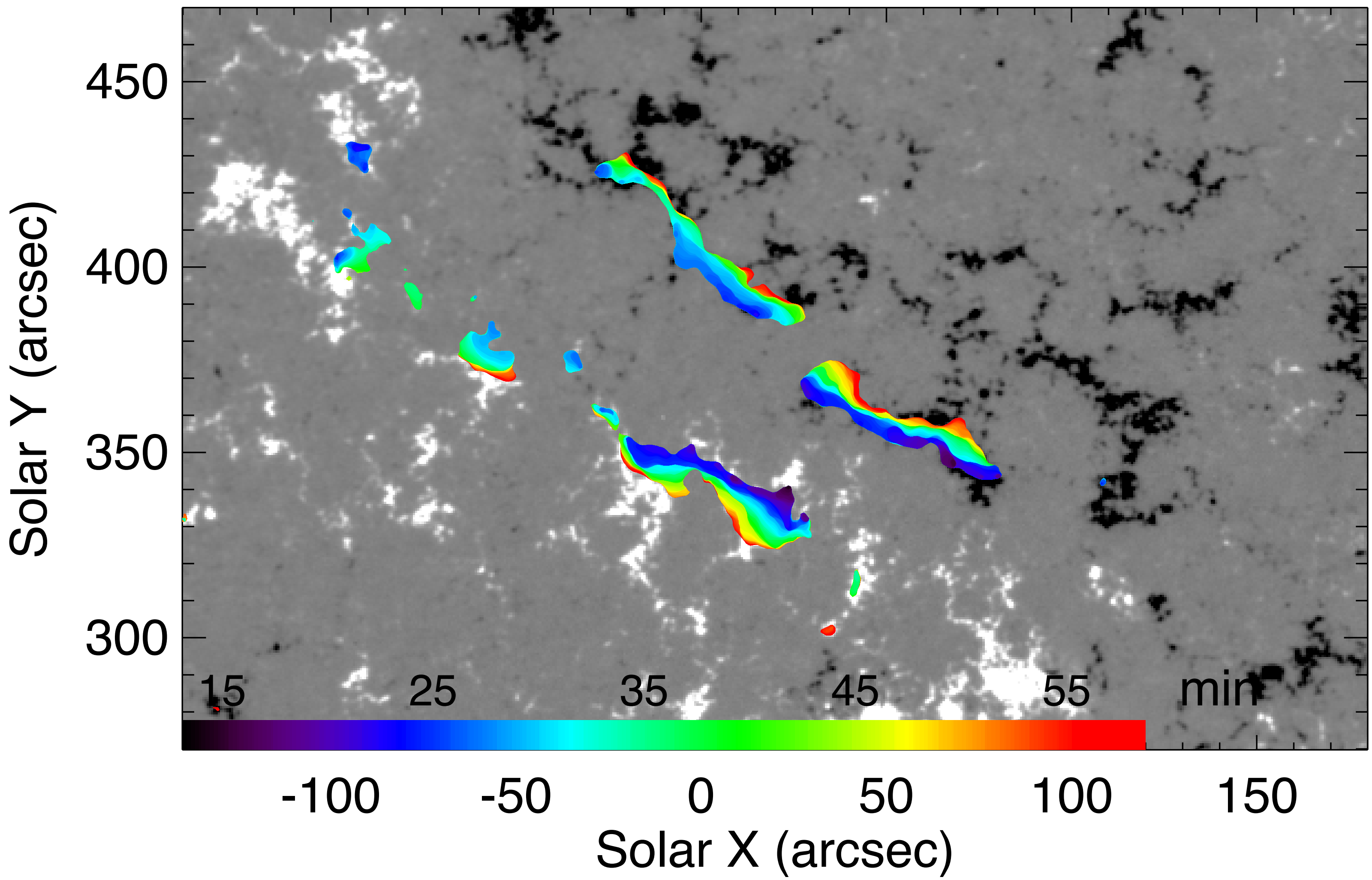


$$\Phi_B = \int B_{in}\, dA_{in} = \int B_R\, dA_R$$

# reconnection flux is a good fraction of the AR flux

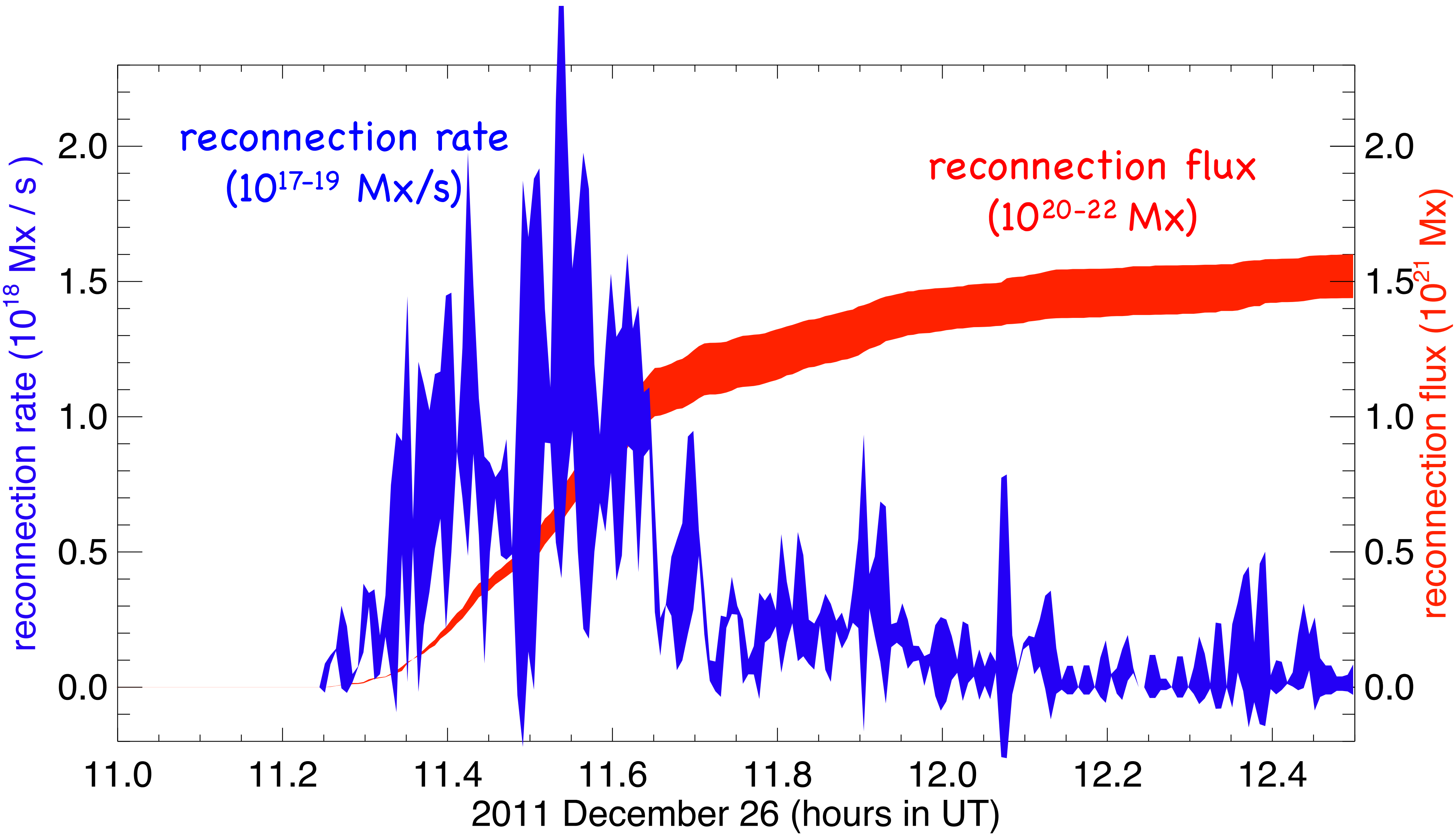


Qiu et al, 2002-2010, Kazachenko et al. (2017)

# toroidal flux from the standard-model

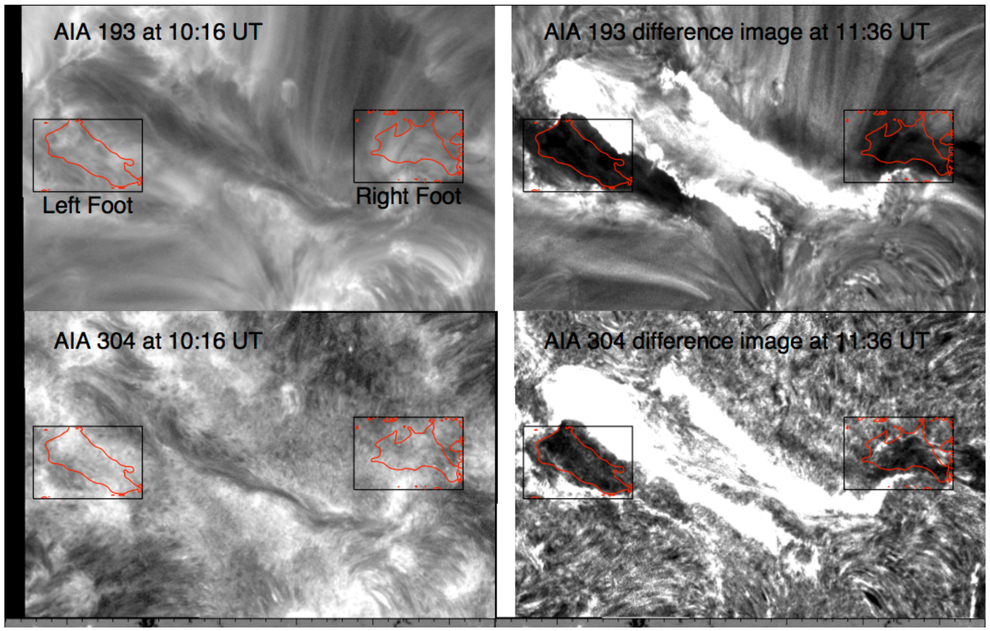


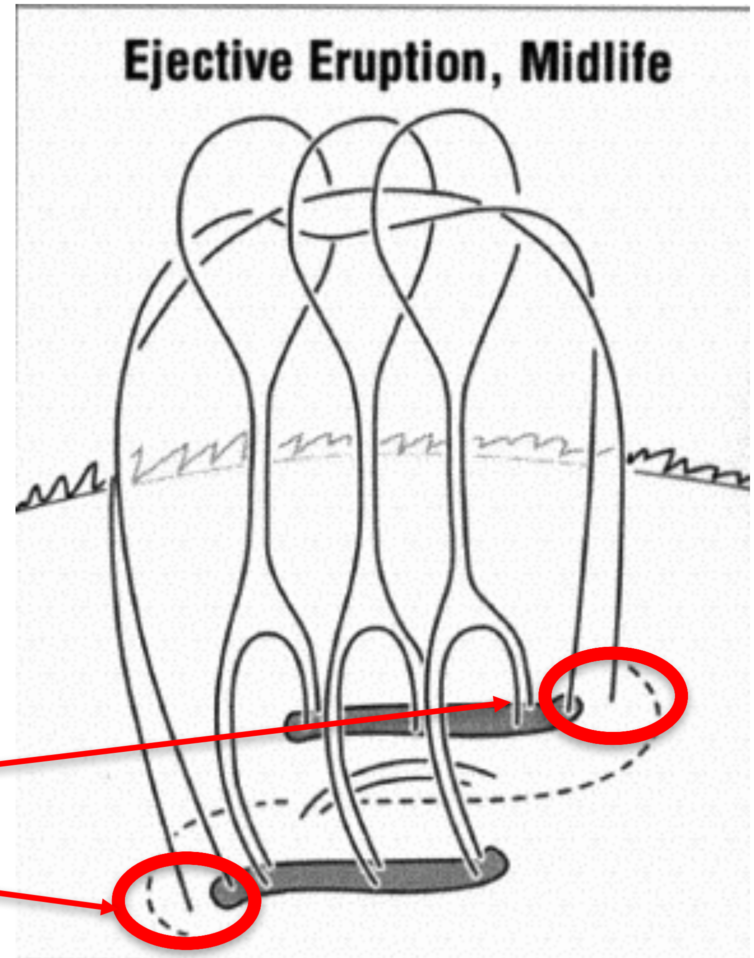


Moore et al. (2001)

The erupting rope causes coronal dimming at the two feet, with which the axial flux of the rope is estimated.

# handedness of reconnection formed flux rope

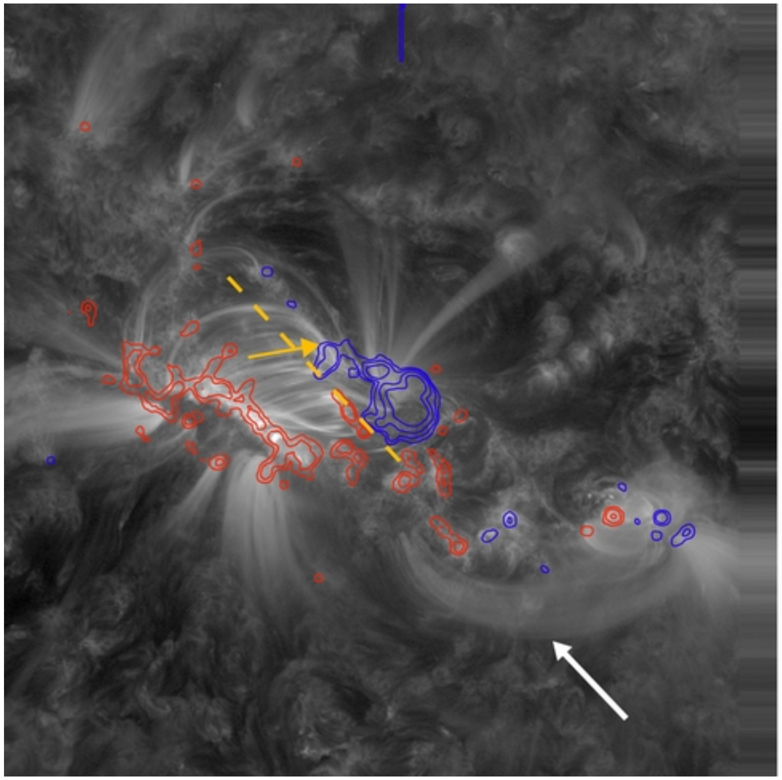

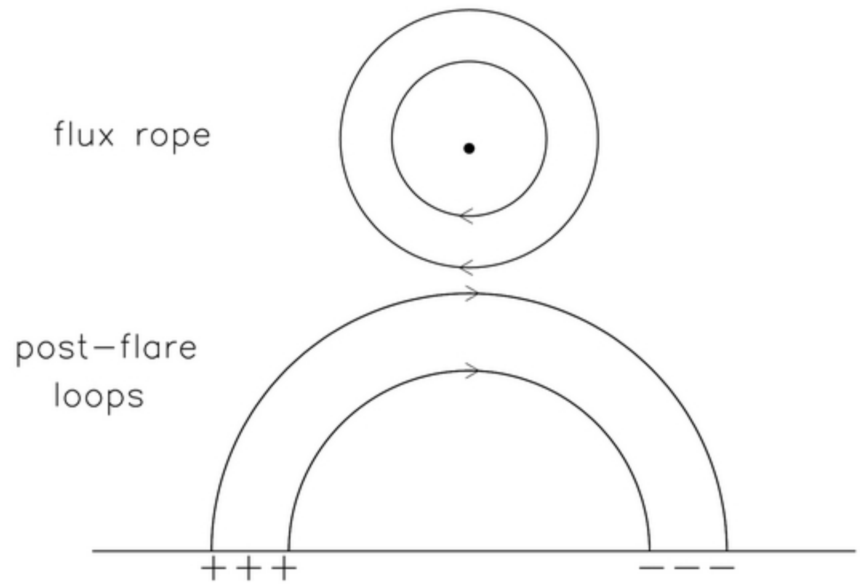


Yurchyshyn et al. 2001, Leamon et al. 2004, Hu et al. 2014

# compare MC and solar signatures

WEBB ET AL.: ORIGIN AND DEVELOPMENT OF MAY 1997 MAGNETIC CLOUD 27,255

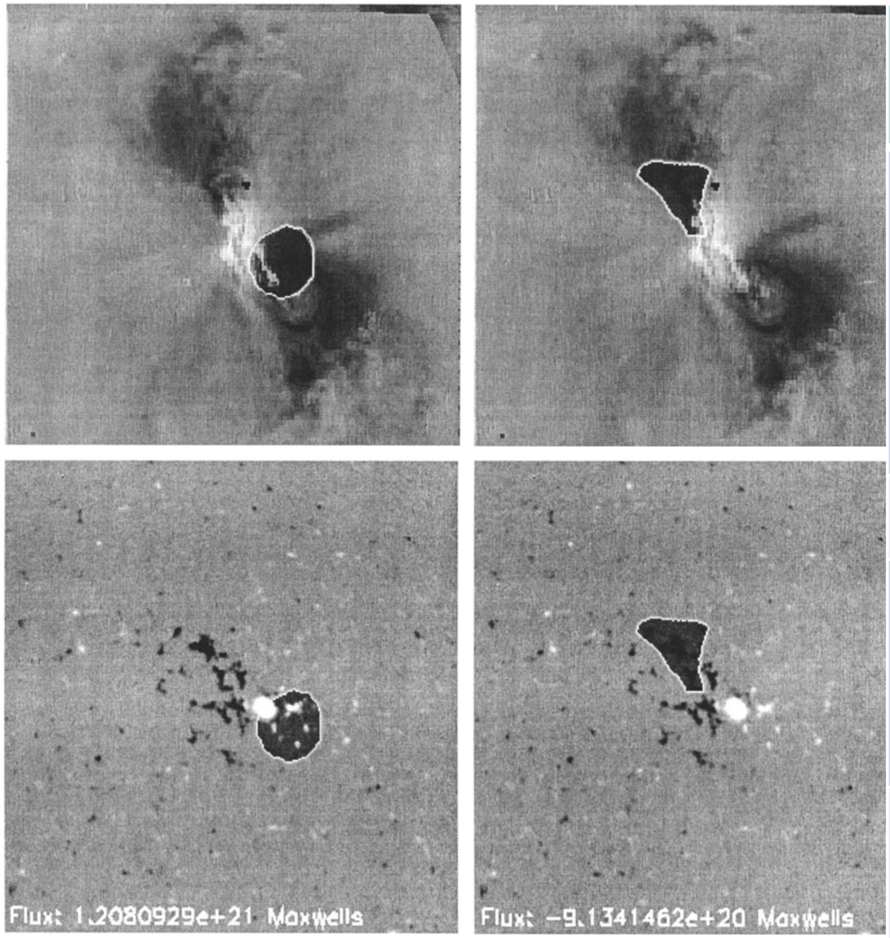


Figure 3. (Top) EIT difference image (0507 UT–0450 UT) and (bottom) MDI image (0454 UT). Superposed are the area masks which were used to estimate total magnetic flux at the assumed footpoints of erupting loop system. Masks used for the southwest (left) and northeast (right) dimming regions.

| parameters | Solar surface signatures | MC flux rope |
|---|---|---|
| Projected orientation | $45^0$ NE of equator<br>$30^0$ - $55^0$ NE (range)<br>$55^0$ axis of dimmings<br>Filament rotates toward E-W | $-11^0$ ecliptic latitude,<br>$108^0$ ecliptic longitude<br>S-E-N type |
| handedness | left | left |
| Magnetic flux | $1.0x10^{21}$ Mx (dimmings) | $7.35x10^{20}$ Mx (axial) |
| speed | 600 km/s (CME front) | 430-500 km/s |

An event on 1997 May 12-15 analyzed by Webb et al. (2000)

# reconnection flux and MC flux

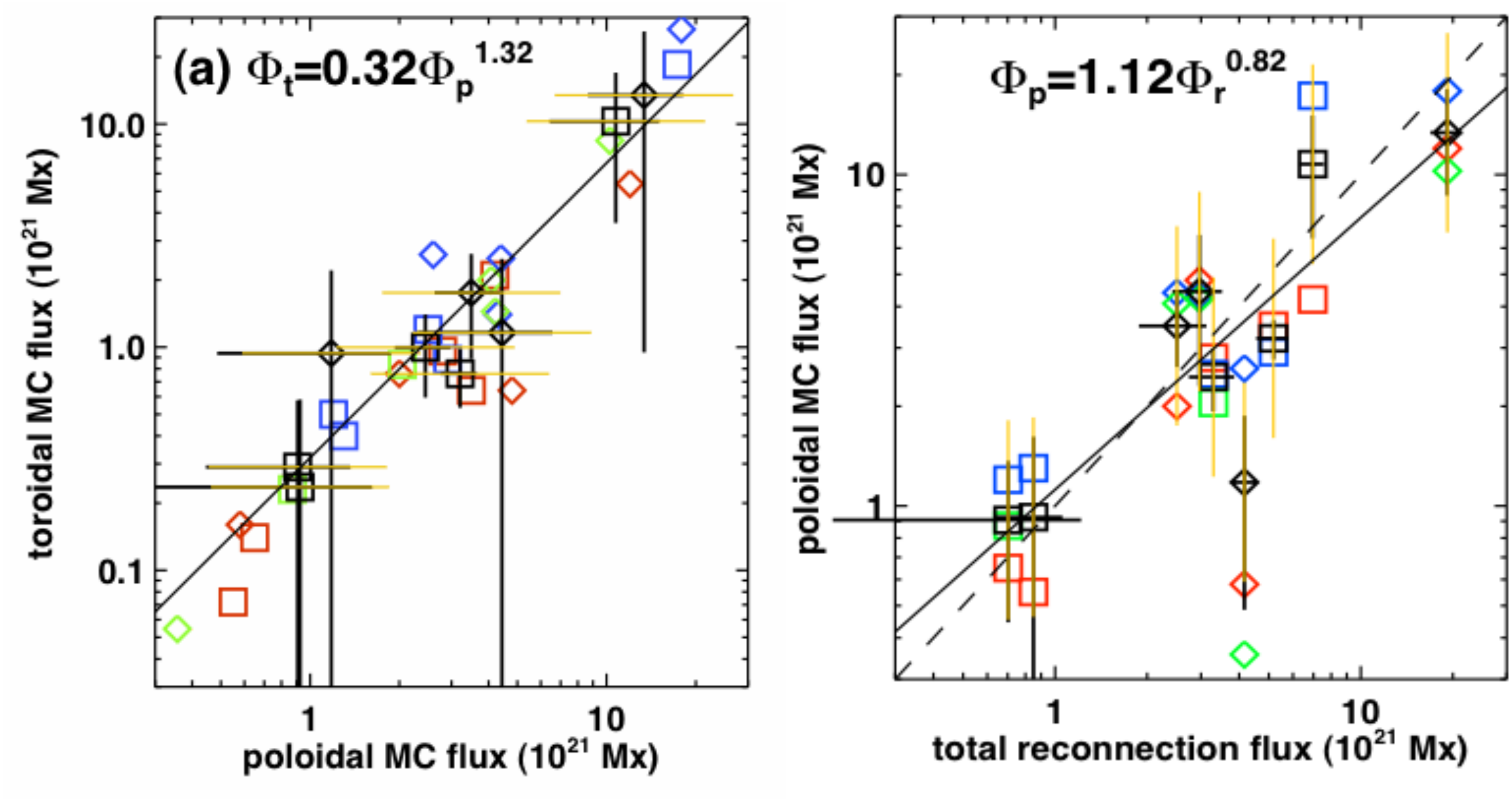


(Qiu et al. 2007, Hu et al. 2014)

# reconnection flux and MC flux

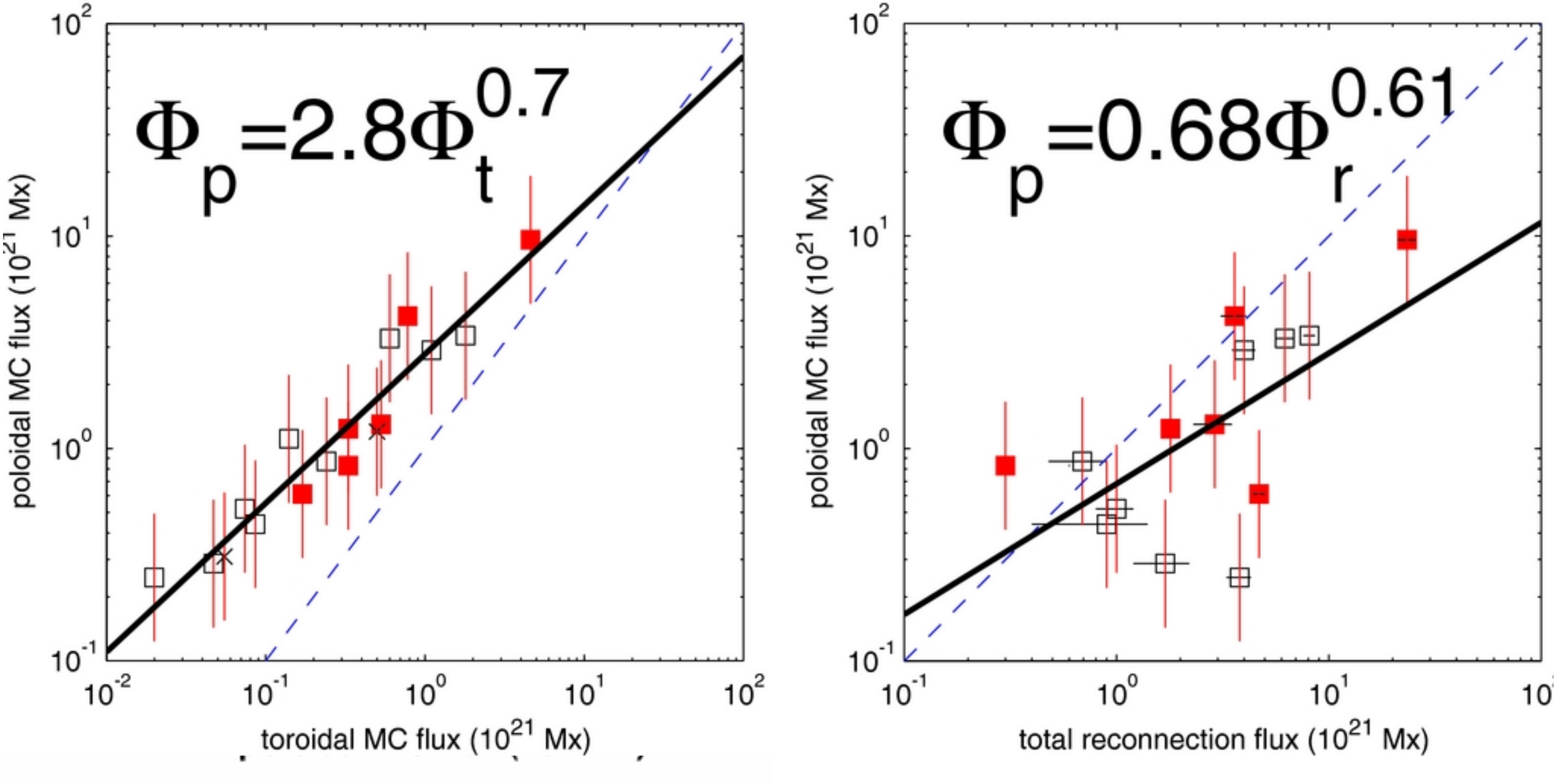


(Qiu et al. 2007, Hu et al. 2014)

# dimming flux and MC flux

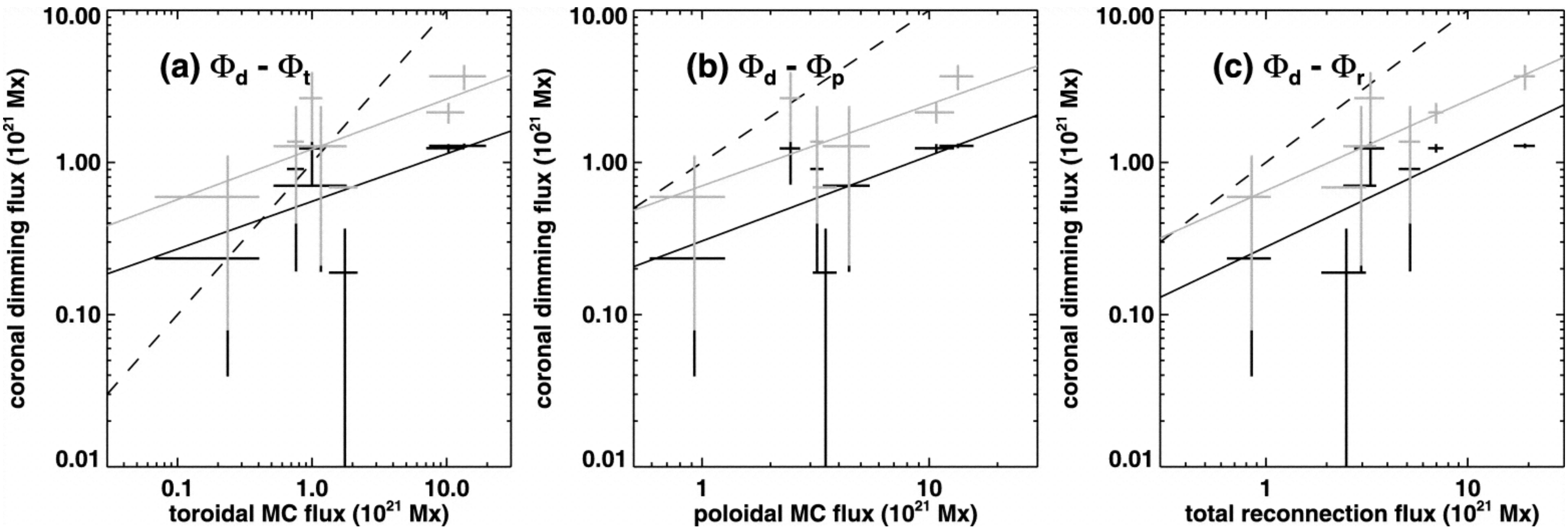


(Qiu et al. 2007)

# flare configuration and MC twist

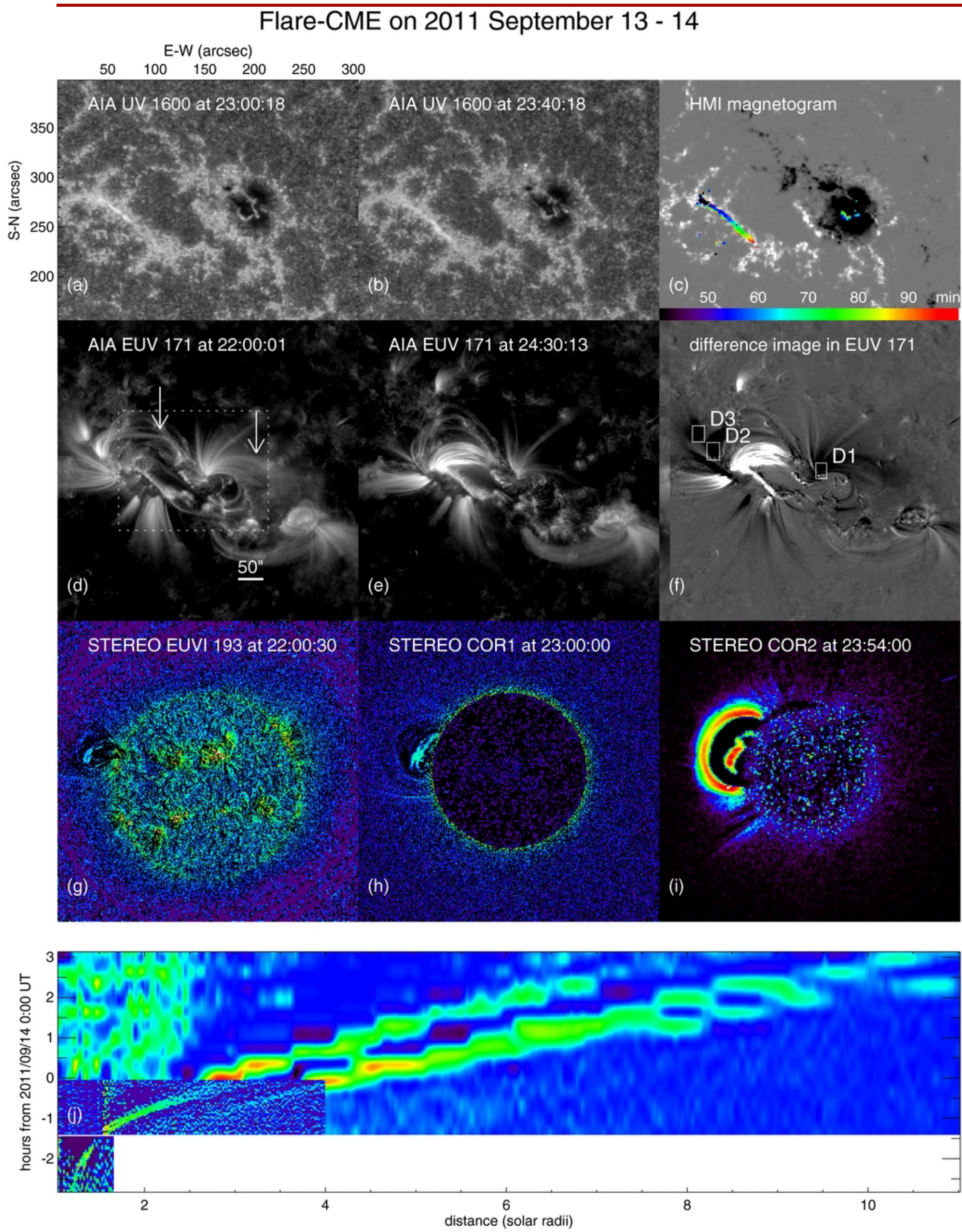


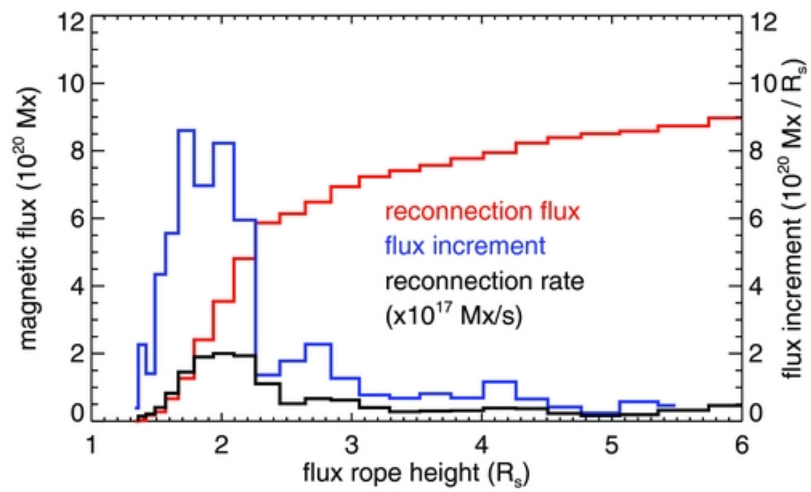


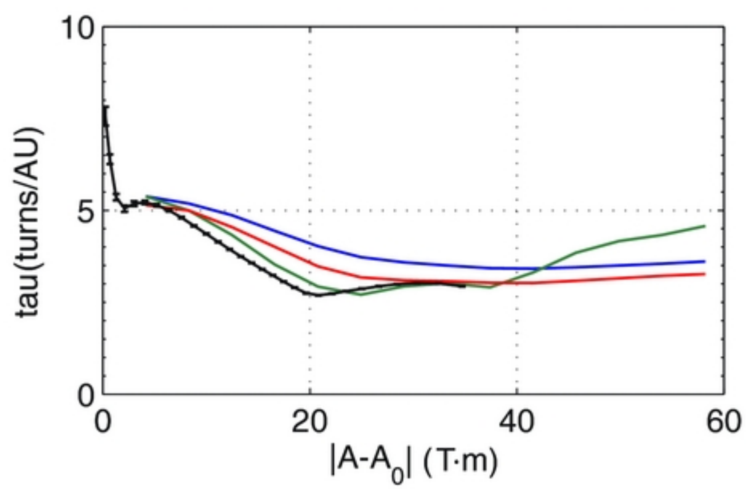


An event with decreasing twist (Hu et al. 2014)

# flare configuration and MC twist

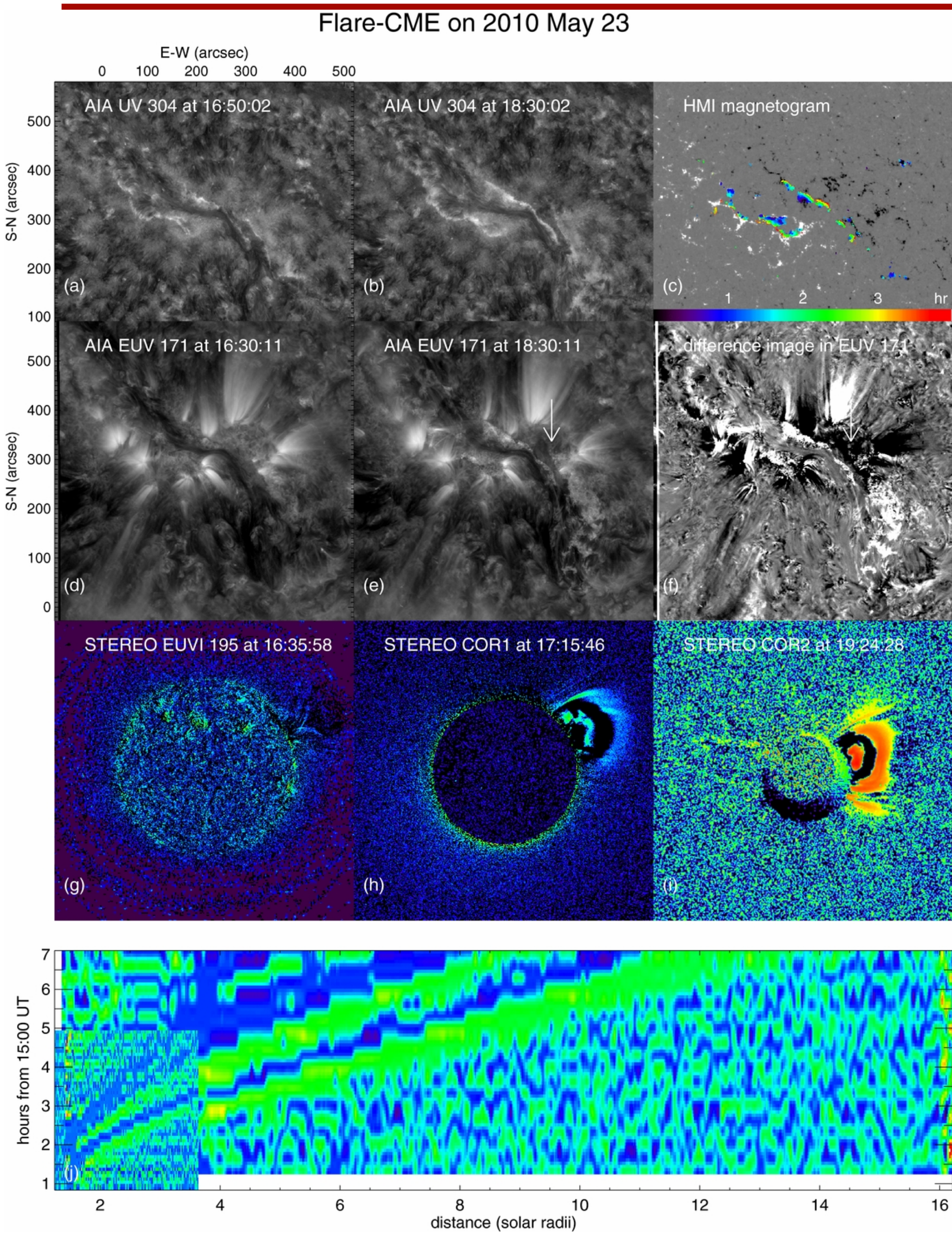


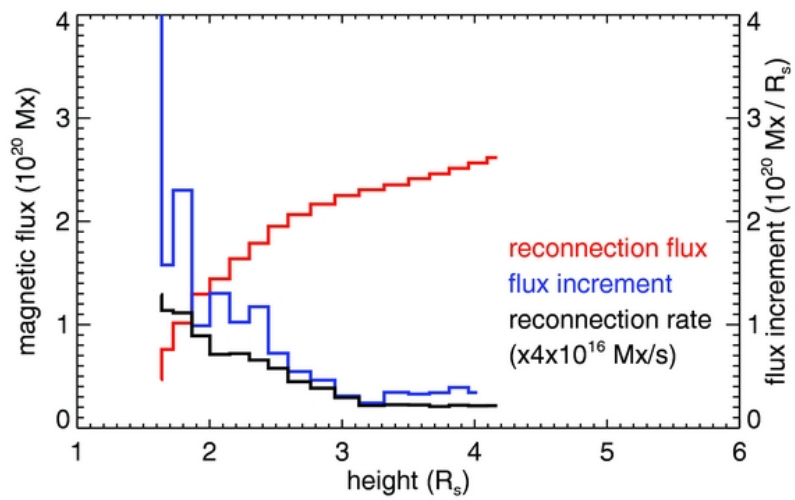


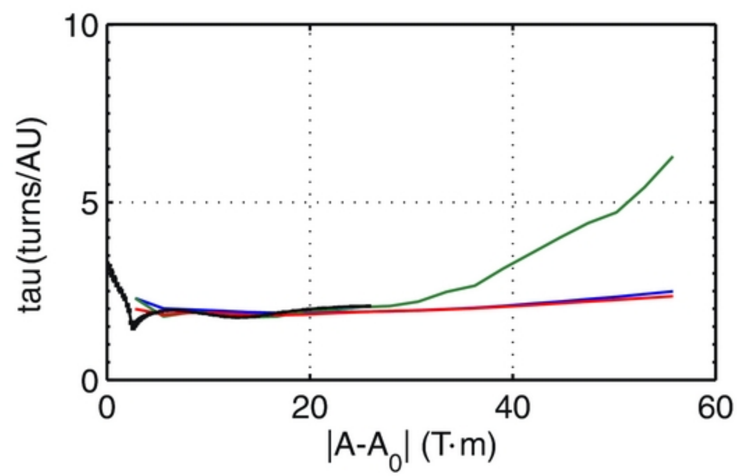


An event with flat twist (Hu et al. 2014)

# flare configuration and MC twist

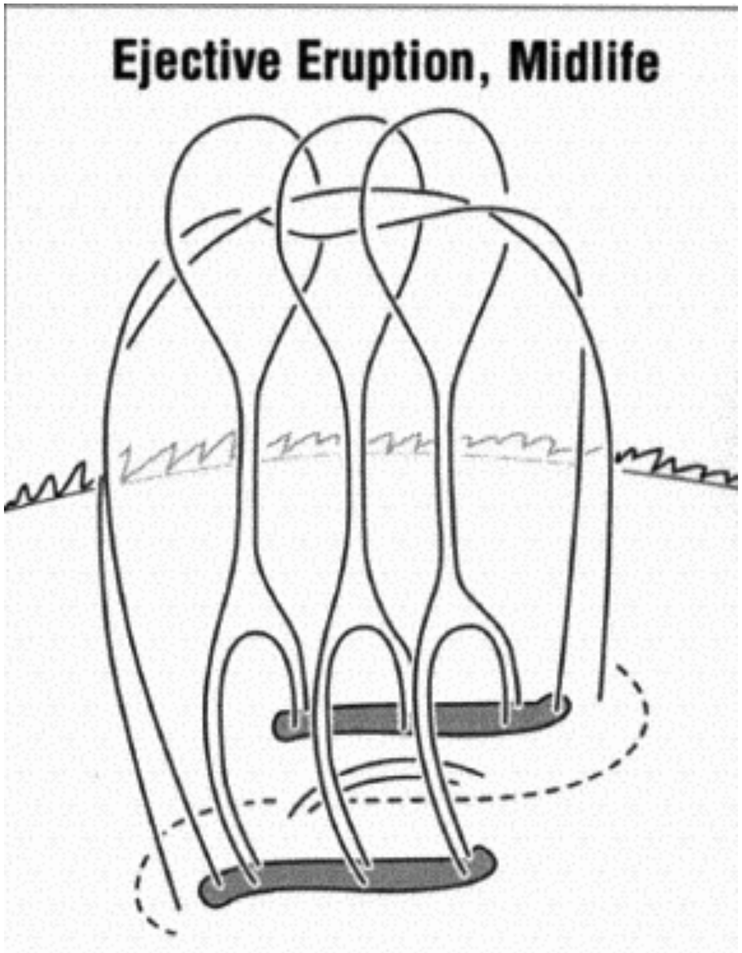


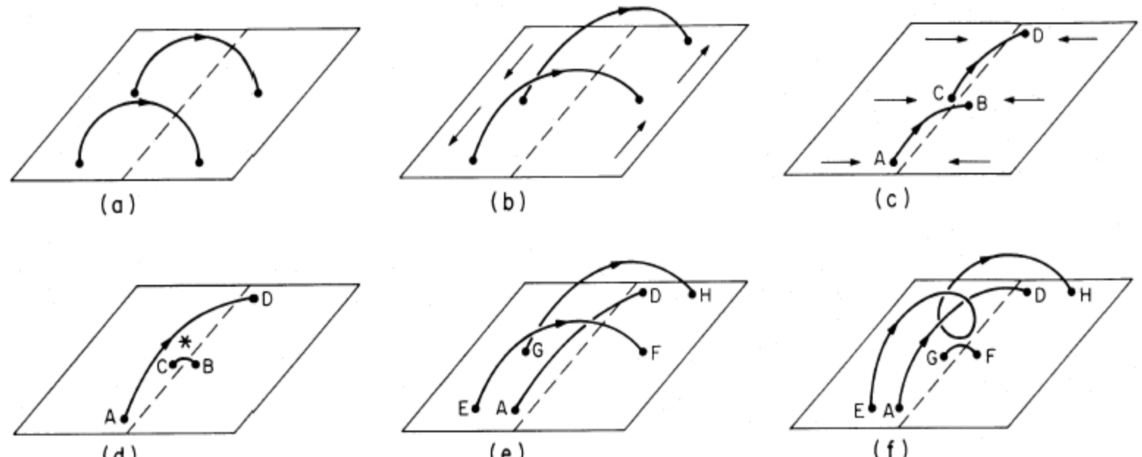


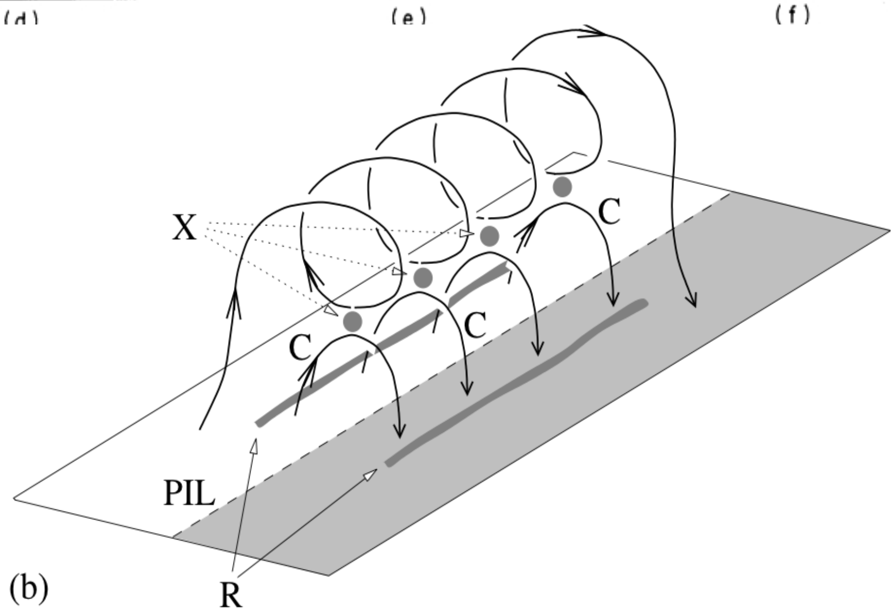


(b)

Which one is correct? What do we see in MC flux rope and flare? (Priest et al. 2016, 2017)

## Summary

MC measurements provide evidence of flux ropes, which probably carry a large amount of twist.

MC flux ropes are formed in the Sun, and reconnection plays an important role in its formation, as well as its energetics.